AN ABSTRACT OF THE THESIS OF

Sarah C. Holm for the degree of Honors Baccalaureate of Science in Civil Engineering presented on June 1, 2007. Title: Location of the Neutral Axis in Wood Beams.

Abstract approved: _____

Thomas H. Miller

_____

Rakesh Gupta

It is commonly accepted that for the analysis of wood beams, the neutral axis coincides with the centroid of the beam. Although this assumption is used in analysis, wood is not an isotropic material, as it has different elastic properties in the tangential, radial and longitudinal directions, nor is it homogenous, as it contains characteristics, such as knots, at various locations in the material. Because of this, there is a need for an analysis of the neutral axis for anisotropic, non-homogenous materials, such as wood, in order to better predict the deformations and strains in such materials. Specifically, with the use of Digital Imaging Correlation, a non-contact technique used to measure the deformation of an object's surface, this project examines how knots in wood influence the location of the neutral axis. The output from the VIC-3D digital imaging correlation software provides a clear image of the location of the neutral axis. From this project it is apparent that the neutral axis in the clear beam remained close to the centroidal axis throughout loading, while the location of a knot within the beam determines the size of the compression and tension zones as well as the location of the neutral axis.

Key Words: Neutral axis, wood, knots, inelastic behavior, anisotropic materials
Corresponding e-mail address: holms@onid.orst.edu

Location of the Neutral Axis in Wood Beams

By

Sarah C. Holm

A PROJECT

Submitted to

Oregon State University

University Honors College

In partial fulfillment of
the requirements for the
degree of

Honors Baccalaureate of Science in Civil Engineering (Associate Honors Scholar)

Presented June 1, 2008
Commencement June 2007

Honors Baccalaureate of Science in Civil Engineering project of Sarah C. Holm presented on June 1, 2007.

APPROVED:

Thomas H. Miller
Mentor, representing Civil Engineering

Rakesh Gupta
Committee Member, representing Wood Science and Engineering

Milo Clauson
Committee Member, representing Wood Science and Engineering

Director, School of Civil and Construction Engineering

Dean, University Honors College

I understand that my project will become part of the permanent collection of Oregon State University, University Honors College. My signature below authorizes release of my project to any render upon request.

Sarah C. Holm, Author

ACKNOWLEDGMENTS

I contribute much of this project's success to my mentors, Dr. Thomas Miller, an Associate Professor in Civil Engineering at Oregon State Univerity, and Dr. Rakesh Gupta, an Associate Professor in Wood Science and Engineering at Oregon State Univerity, my committee member, Milo Clauson, a Senior research Assistant in Wood Science and Engineering at Oregon State Univerity and Arijit Sinja, a graduate student in Wood Science and Engineering at Oregon State Univerity. I appreciate all your support and encouragement throughout the completion of this project.

TABLE OF CONTENTS

LIST OF FIGURES

LIST OF FIGURES (Continued)

LIST OF FIGURES (Continued)

LIST OF TABLES

LIST OF APPENDICES

Location of the Neutral Axis in Wood Beams

1.0 INTRODUCTION

The neutral axis for a beam is defined as the line in the cross-section where there is neither longitudinal compression nor tensile stress, as shown in Figure 1.1. It is commonly accepted that for the analysis of wood beams, the neutral axis coincides with the centroid of the beam. Although this assumption is used in analysis, wood is not an isotropic material, as it has different elastic properties in the tangential, radial and longitudinal directions, nor is it homogeneous, as it contains characteristics, such as knots, at various locations in the material. Therefore, there is a need for an analysis of the behavior of the neutral axis for wood beams.

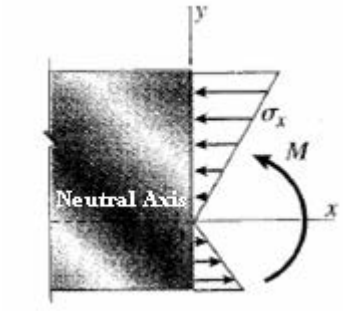

Figure 1.1: Neutral Axis of a Beam in Bending (Gere and Timoshenko 1997)

1.1 Objective

The purpose of this project is to examine the validity of the previously stated assumption for an anisotropic, non-homogeneous wood beam. Specifically, it will examine how knots in the wood influence the location of the neutral axis. Because the neutral axis of beams is well-defined for isotropic, homogeneous materials, there is a need for an analysis of the neutral axis for anisotropic, non-homogeneous materials, such as wood, in order to better predict the

deformations and strains in such materials, as well as provide a better estimation of the mechanical properties of wood.

1.2 Personnel

This project was conducted by Sarah Holm, an undergraduate student in Civil Engineering at Oregon State University along with a team consisting of Dr. Thomas Miller, a Structural Engineering professor at Oregon State University, Dr. Rakesh Gupta, a Wood Science and Engineering professor at Oregon State University, and Milo Clauson, a Senior Faculty Research Assistant in the Wood Science and Engineering Department at Oregon State University.

1.3 Expected Results and Significance

The standard location of the neutral axis in beams may not be accurate for anisotropic and non-homogeneous wood beams, and thus current deformation analyses for wood beams may be somewhat incorrect as well. The projected outcome of the project is to provide a better understanding of the deformation and stiffness of wood beams. Additionally, this project could lead to improved deformation analysis of other anisotropic and non-homogeneous materials in the future.

1.4 Methodology

This research project will first examine the location of the neutral axis of a relatively clear or straight-grained piece of wood in pure bending. Similar research has been performed on other materials such as high strength concrete and composite steel plates. This project will examine how knots affect the location of the neutral axis in a non-homogeneous wood beam.

Testing will be accomplished using Digital Image Correlation (DIC) equipment to determine the strains and deformations of the beam. DIC takes a series of images of a small area during an applied loading. The images depict the deformation relative to the undeformed shape. The deformations can be used to determine the strains. Strain contour plots can be used to determine where the neutral axis is located. The results of these tests may show that the standard location of the neutral axis in beams may not be accurate for anisotropic and non-homogeneous wood beams, and thus current deformation analyses for wood beams may be somewhat incorrect as well. The projected outcome of the project is to provide a better understanding of the deformation and strength of wood beams.

2.0 LITERATURE REVIEW

2.1 Beam Theory

In order to begin this project, it is necessary to understand elastic and inelastic beam behavior for both homogeneous and non-homogeneous beams.

2.1.1 Elastic Behavior

Elasticity describes behavior in which deformations caused by low stresses are completely recoverable once the loading is removed. At higher stresses, plastic behavior occurs in which deformations will not recover after loading. Gere and Timoshenko (1997) explained that in a simply supported beam subjected to bending, the longitudinal stresses are greater in the middle of the length and at the extreme edges above and below the neutral axis. The neutral axis is the dividing line between the region of the beam in tension and the region in compression. During bending, the neutral axis does not change in length. It is assumed that the material properties and dimensions, of the undeformed beam are symmetric about the plane of bending, or the x-z plane shown in Figure 2.1. The neutral axis is located along the x-axis of the beam when it exhibits elastic behavior. It is also assumed that in pure bending all cross sections remain plane during loading. Figure 2.1 shows an element, dA, that is y away from the neutral axis. We can determine the location of the element from the neutral axis from Equation 2.1.

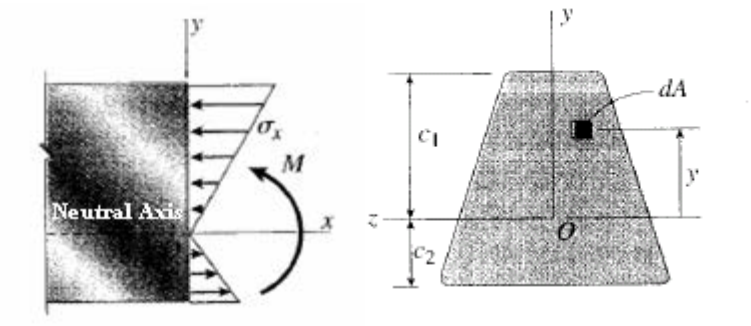

(a) (b)

Figure 2.1: Normal stresses in a beam of linearly elastic material (a) side view (b) Cross section where x-z plane is neutral surface (Gere and Timoshenko 1997)

$$\int_A y dA = 0 \qquad \textbf{(Equation 2.1)}$$

This equation shows that the first moment of area of the cross-section of the beam evaluated with respect to the z-axis is equal to zero. This means that the x-axis must pass through the centroid of the cross-section. Therefore, as long as the material behavior is linearly elastic and its dimensions are symmetric about the centroidal axis, the neutral axis will pass through the centroid of the cross-sectional area as well since it lies on the z-axis. In addition, Gere and Timoshenko (1997) describe the location of the neutral axis by examining a longitudinal line at any location on the beam. Because this line moves with the beam during bending, as does the neutral axis, it is assumed that the distance between the line and the neutral axis remains the same. Gere and Timoshenko describe the longitudinal strain of this line by Equation 2.2:

$$\varepsilon_x = -\frac{y}{\rho} = -\kappa y \qquad \textbf{(Equation 2.2)}$$

Where κ is the curvature of the beam and ρ is the radius of curvature. This equation shows that the longitudinal strains in the beam vary linearly with the distance y from the neutral

axis. Furthermore, Gere and Timoshenko explain that this linear relationship is true independent of the shape of the stress-strain curve of the material.

2.1.2 Inelastic Behavior

As loading is continued, the yield stress of the material is reached and the behavior of the beam becomes inelastic. As shown in Figure 2.2, during inelastic bending, the top and bottom of the member reach yield stress while the center has not yet yielded and remains elastic. Finally, when the entire section has yielded, the entire beam exhibits completely plastic behavior.

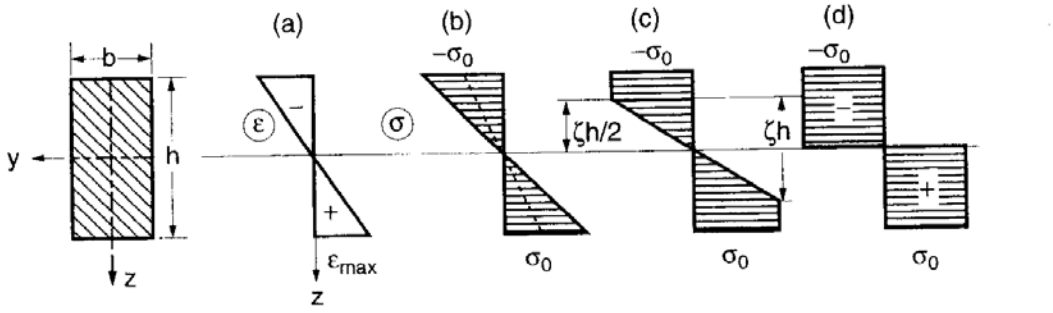

Figure 2.2: Rectangular cross section under pure bending: a) strain distribution, b) stress at the elastic limit state, c) stress at an elastoplastic state, d) stress at the plastic limit state (Bažant and Jirásek 2002)

For beams in which the tension and compression zones are different, the neutral axis will only lie on the centroidal axis when the beam is in the elastic region. However, when the beam begins to experience inelastic behavior, the material will begin to yield first on either the top or bottom of the height of the beam and the neutral axis will move up or down depending on whether the material has a higher tension or compression capacity. This is shown in Figure 2.3.

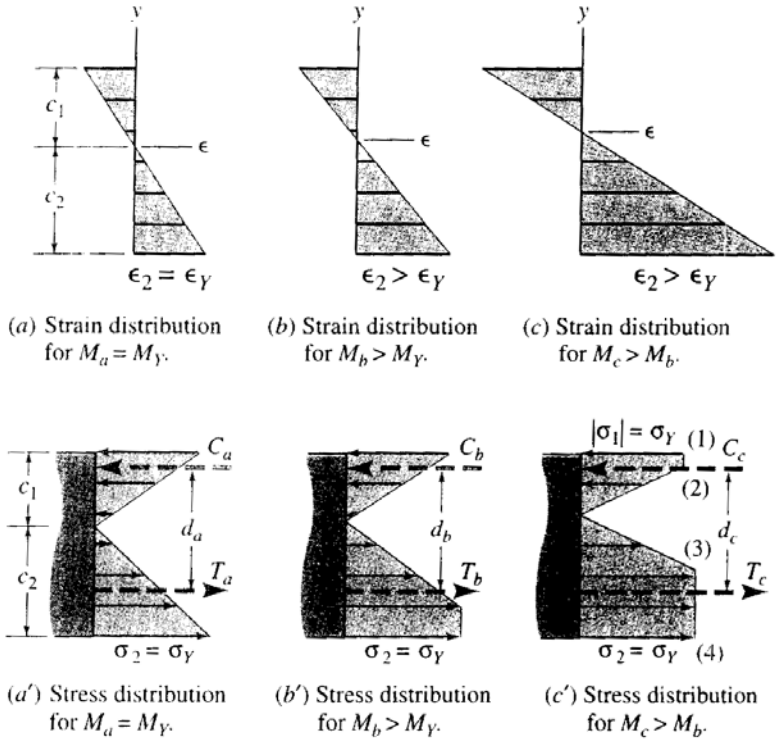

Figure 2.3: Strain and stress Distribution for an Elastic-Plastic Beam (Craig 1996)

This relates to wood because wood has different strength capacities in compression and in tension. Additionally, knots affect the strength capacities of the beam even more depending on their location. For example, for a beam in bending with a knot located in the bottom of the beam, the tensile strength will be greatly reduced and therefore the bottom side of the beam will yield first, before the top of the beam. Therefore, it can be expected that the neutral axis will move up or down depending on the location of the knot.

2.1.3 Anisotropic Materials

Boresi et al. (1993) define anisotropic materials as those that exhibit different independent elastic properties in different directions. The inelastic behavior of anisotropic materials is complicated but can be simplified by assuming the material is orthotropic, having different properties in three mutually perpendicular directions. Bažant and Jirásek (2002) define the

yield criterion as the stress states for which a material exhibits plastic flow. Anisotropic materials are described by their moduli of elasticity and their yield criterion. The Hoffmann yield criterion best reflects wood because it models the material with different yield stresses in tension and in compression.

Bažant and Jirásek explain that the Hoffmann yield criterion defines the orthogonal axes as x_1, x_2, and x_3 and the stress components with respect to the corresponding axes of orthotropy as σ_{11}, σ_{12} etc. For example, the parameter σ_{12}^{0+} represents the tensile yield stress with respect to the x_1 and x_2 axes. The Hoffman criterion is as follows:

(Equation 2.3)

$$\left(\frac{\sigma_{22}-\sigma_{33}-c_{22}+c_{33}}{k_{11}}\right)^2+\left(\frac{\sigma_{33}-\sigma_{11}-c_{33}+c_{11}}{k_{22}}\right)^2+\left(\frac{\sigma_{11}-\sigma_{22}-c_{11}+c_{22}}{k_{33}}\right)^2+\left(\frac{\sigma_{23}}{k_{23}}\right)^2+\left(\frac{\sigma_{31}}{k_{31}}\right)^2+\left(\frac{\sigma_{12}}{k_{12}}\right)^2-1=0$$

Where c_{11},c_{22}, c_{33} correspond to the shifted center of the yield surface and:

$$c_{11}=\frac{\sigma_{11}^{0+}-\sigma_{11}^{0-}}{2},\qquad c_{22}=\frac{\sigma_{22}^{0+}-\sigma_{22}^{0-}}{2},\qquad c_{33}=\frac{\sigma_{33}^{0+}-\sigma_{33}^{0-}}{2}$$ **(Equation 2.4)**

And, where the k values are material parameters, and for uniaxial tension along the x_1 axes they can be expressed by:

$$k_{11}=\sqrt{2}\left(\frac{1}{(\sigma_{22}^0)^2}+\frac{1}{(\sigma_{33}^0)^2}-\frac{1}{(\sigma_{11}^0)^2}\right)^{-1/2}$$ **(Equation 2.5)**

Analogous expressions for k_{22} and k_{33} can also be computed, and for pure shear in the x_1-x_2 plane, where τ^0_{12}, τ^0_{23}, and τ^0_{31} represent the shear stresses for the each plane:

$$k_{12}=\tau_{12}^0,\qquad k_{23}=\tau_{23}^0,\qquad k_{31}=\tau_{31}^0$$ **(Equation 2.6)**

2.1.4 Ductility

Ductility can be defined as the capacity of a material to deform permanently under stress or the energy absorbed by the material until fracture. Lopes and Bernardo (2004) define ductility as the ability of a beam to be subjected to excessive plastic deformation without a great loss of its resistance. It is also measured by the area under the stress versus strain curve. A very ductile material can withstand local stress concentrations. Ductility, μ, can be represented by Equation 2.7:

$$\mu = \frac{\Delta_{max}}{\Delta} \qquad \textbf{(Equation 2.7)}$$

Because the neutral axis moves away from the centroidal axis as the beam behaves inelastically, ductility is maintained by keeping the distance from the centroid to the neutral axis small at failure. The neutral axis position is defined by the parameter x/d, where x is the depth of the neutral axis, and d is the effective depth of the beam.

2.2 Mechanical Properties of Wood

Wood is a very anisotropic material, meaning that the modulus of elasticity is different in different directions. To simplify, wood is also an orthotropic material because it has different properties in three mutually perpendicular directions, the radial, tangential and longitudinal principle axes as shown in Figure 2.4.

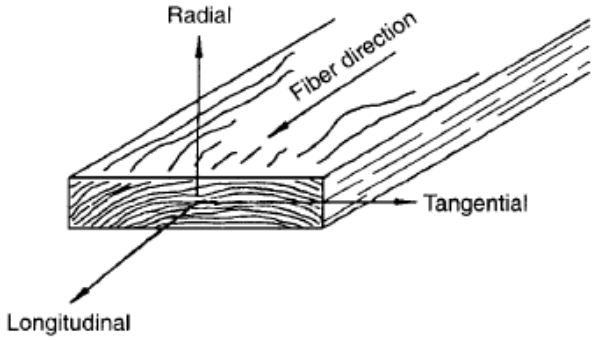

Figure 2.4: Three Principal Axes of Wood with Respect to Grain Direction and Growth Rings (Forest Products Laboratory 1999)

Clear wood is much stronger in tension than in compression. In fact, according to the Forest Products Laboratory (1992), the tensile strength of clear wood parallel to the grain is approximately 100,000 kPa while the compressive strength parallel to the grain is about 50,000 kPa. Therefore, as seen in Figure 2.5, the tensile stresses below the neutral axis of a simply supported wood beam subjected to bending may be twice that of the compressive stresses above the neutral axis at failure. The Forest Products Laboratory also notes that the behavior of wood subjected to tensile stresses (parallel to the grain) is nearly elastic right up to failure. However, wood in compression parallel to the grain fails by instability of the submicroscopic structure, and as stresses increase throughout the structure the instability of the submicroscopic structure continues with folding of wood cells until failure.

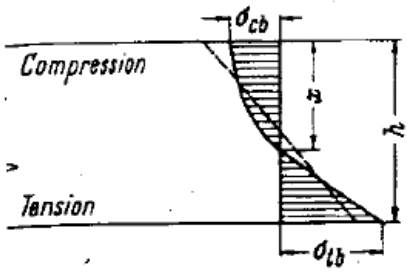

Figure 2.5: Stress-Strain Diagram for Cross-Section of Clear Wood Beam (Kollmann and Cote 1968)

Wood beams in bending most commonly fail on the compressive side first. This failure increases the compressive stresses in the beam until the tensile failure stress is achieved, and then the entire beam fails. The Forest Products Laboratory states that the characteristic bending strength for wood is approximately 75,000 kPa. The bending strength is represented by the modulus of rupture, or the stress at the extreme fiber of the beam explained by Equation 2.8, which is calculated from the maximum bending moment assuming an ideal stress distribution.

$$\sigma = \frac{Mc}{I} \qquad \textbf{Equation 2.8}$$

The moment, M, is calculated from the statics of the load and beam geometry, c, is the distance from the neutral axis at the extreme compression fiber and the moment of inertia, I, is calculated from the beam geometry. Somayaji (2001) explains that lumber in bending only behaves elastically initially and then behaves inelastically up until failure. This can be seen in Figure 2.6. Therefore, calculations that assume elastic behavior for wood beams do not truly describe the actual inelastic behavior and movement of the neutral axis in lumber. In order to perform a correct stress analysis we would need to assume inelastic behavior for the wood beam as explained above in the Beam Theory section.

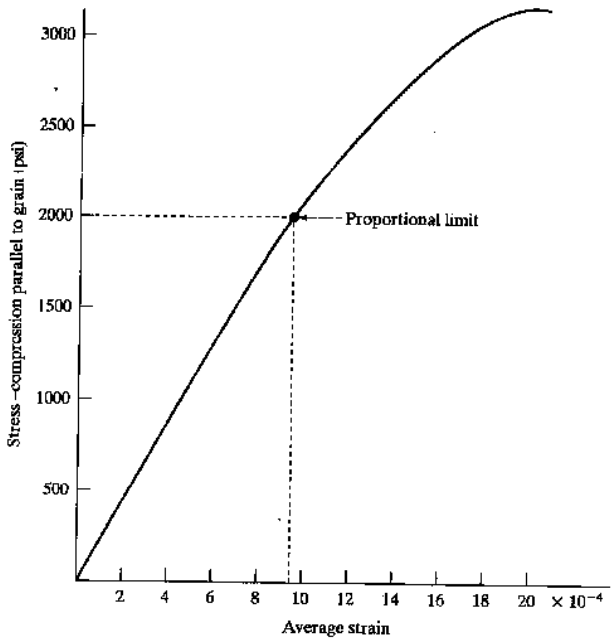

Figure 2.6: Typical Stress-Strain Diagram of Lumber (Compression Parallel to the Grain) (Somayaji 2001)

Kollmann and Cote (1968) explain that for an idealized trapezoidal distribution of the stresses in a wood beam in bending, as shown in Figure 2.7, the location of the neutral axis can be determined by Equation 2.9.

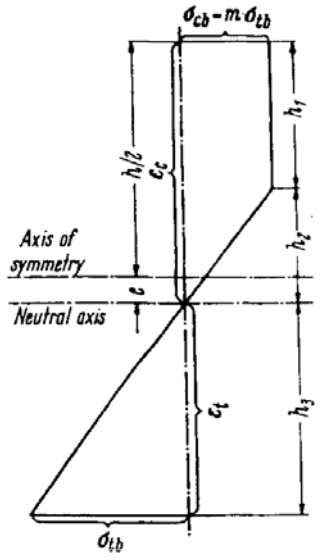

Figure 2.7: Stress Diagram for Trapezoid-like Distribution of the Stresses Over the Cross-Section of a Wood Beam (Kollmann and Cote 1968)

$$\frac{x}{h} = \frac{1+m^2}{(1+m)^2} \qquad \text{Where:} \qquad m = \frac{\sigma_{cb}}{\sigma_{tb}} \qquad \textbf{Equation 2.9}$$

Here, x is the distance from the top of the beam to the neutral axis, h is the height of the beam, and m is equal to the ratio of the crushing strength to the tensile strength. As shown in Figure 2.7, for clear beams, the neutral axis should be expected to be below the centroidal axis. Additionally, from Equation 2.9, for a clear wood beam in bending where the tensile strength is assumed to be equal to twice that of the compressive strength, the m is equal to 0.5, and therefore the position of the neutral axis is assumed to be at x/h = 0.556. Kollmann and Cote show that using the idealized trapezoidal stress distribution for wood beams, Equation 2.10 holds true.

$$\varepsilon_{cb} = \frac{\sigma_{tb}}{E} \cdot \frac{1+m^2}{2m} \quad or \quad \frac{\varepsilon_{cb}}{\varepsilon_{tb}} = \frac{1+m^2}{2m} \qquad \textbf{Equation 2.10}$$

In Equation 2.10, ε_{cb} and ε_{tb} represent the compressive and tensile strains in the beam in bending, respectively, and σ_{cb} and σ_{tb} represent the compressive and tensile stresses in the beam in bending, respectively. This can also be used to determine the location of the neutral axis depending on the ratio between the strains in the compression and tensile zones. Again, both Equation 2.9 and Equation 2.10 apply for beams in bending under elastic behavior.

Mechanical properties most commonly vary with the species, differences within species, and characteristics of the wood. Wood is strongest when the stresses are applied parallel to the direction of greatest strength in the member, or the longitudinal direction. Characteristics such as cross grain cause the largest stresses to be at an angle to the grain, lowering the maximum allowable stress.

Knots affect the mechanical properties of wood because they disrupt the direction of the wood fibers around the knot causing cross grain within the beam. Because of this disruption, stress concentrations develop and the mechanical properties are lower in such beams containing knots than in clear wood beams. This is important because sufficient ductility is needed to redistribute these stress concentrations in order to prevent failure. Although wood has a high tensile strength, it fails in a brittle mode when subjected to tensile stresses. On the other hand, despite the low compressive strength of wood, it is more ductile during compressive loading. Kollmann and Cote (1968) noted that knots also reduce the elastic properties, such as the modulus of elasticity, of wood.

The effect of knots depends on their size, location within the beam, shape, soundness and type of stress. Somayaji uses a strength ratio, the ratio of the modulus of rupture of the beam with a reduced cross-section to that of the full beam, to determine the effect of the location of edge knots on a wood beam in bending:

$$strength\ \ ratio = \left(1 - \frac{k}{h}\right)^2 \qquad \textbf{(Equation 2.11)}$$

Here, k is the height of the edge knot and h is the beam depth. This is shown in Figure 2.8.

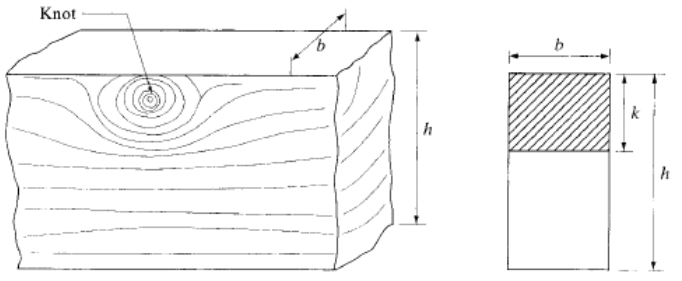

Figure 2.8: Edge knot in a beam (Somayaji 2001).

Equation 2.11 and Figure 2.8 show that the deeper the edge knot is located within the beam, the more the knot will decrease the strength of the wood.

The Forest Products Laboratory (1999) explained that knots affect the strength of wood much more in axial tension than in axial compression. Consequently, the case of a simply supported beam with a knot located below the neutral axis, where the beam is in tension, will have a greater effect on the strength of the beam than a knot located above the neutral axis in compression. Kollmann and Cote (1968) determined that a piece of wood containing a small knot had about fifty percent less tensile strength than that of a clear piece of wood. The Forest Products Laboratory added that the allowable tensile stresses in wood containing knots can be less than the allowable compressive stresses. Knots located on the neutral axis will have very little influence on the strength of the beam. In fact, small knots located on the neutral axis can even increase strength by providing shear resistance.

2.3 Related Works

Lopes and Bernardo (2004) studied the movement of the depth of the neutral axis in high-strength concrete beams subjected to pure bending. The study tested 19 high-strength concrete beams subjected to two equal concentrated loads placed symmetrically at third points of the span, shown in Figure 2.9, to determine whether the depth of the neutral axis at failure in high-strength concrete beams should be limited as it is for normal-strength concrete beams. The neutral axis is limited in order to maintain the ductility within the beam, so that at failure, the depth of the neutral axis from the top of the beam is small. The beams tested were underreinforced to provide plastic behavior and ductility. Using strain gauges and linear transducers, Lopes and Bernardo measured the strain in the beam throughout loading

and plotted load versus deflection curves. The tests showed the depth of the neutral axis rises as the longitudinal tensile reinforcement ratio rises. The neutral axis rises up away from the centroidal axis when cracks develop and when the tension steel begins to yield and the beam behaves plastically until failure. Additionally, the neutral axis moves below the centroidal axis as the beam's ductility decreases.

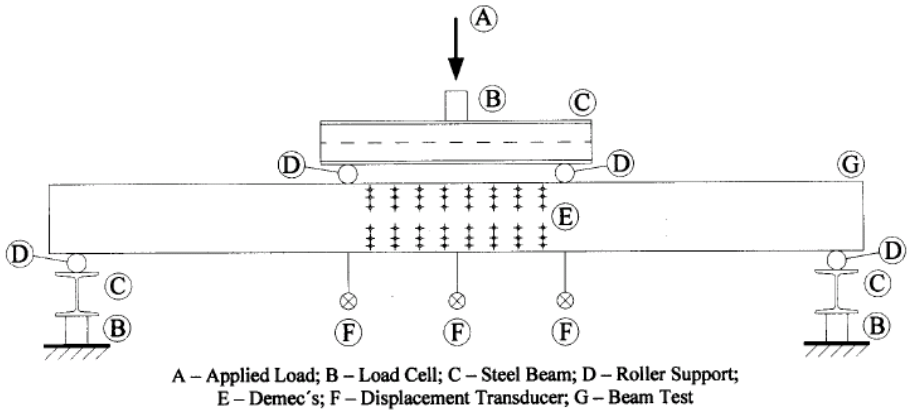

Figure 2.9: Typical test set-up for beam specimen (Lopes and Bernardo 2004).

This is related to the focus of this paper because like wood, reinforced concrete is an anisotropic material. In a clear wood beam subjected to pure flexure, we can expect that the neutral axis will fall below the centroidal axis when the beam behaves inelastically. The movement of the neutral axis during plastic behavior is described by the Hoffman yield criteria as explained previously. However, the tension and compression zones will be different for wood than for reinforced concrete beams, and this will determine how far the neutral axis will move. The neutral axis will move depending on the capacity of the member in compression and tension. Because clear wood beams have approximately a two to one ratio of tensile to compressive strength, the neutral axis will fall below the centroidal axis at failure. Additionally, just as the location of the neutral axis in concrete depends on the modular ratio, or the ratio of the modulus of elasticity of the concrete to that of the steel, the

neutral axis for wood can also be expected to be dependent on the ratio of the modulus of elasticities for the compressive zones and tensile zones. Moreover, as stated previously, a lumber beam containing a small knot would have about fifty percent less tensile strength than a piece of clear wood. Although the effect of the knot depends on its location within the beam and its size, this would mean that the neutral axis would move even further above the centroidal axis during bending.

Yakel and Azizinamini (2005) conducted a study to develop an alternative to the AASHTO method of determining the positive bending moment capacity of composite concrete girders often used for bridges. Using the criteria of Rotter and Ansourian (1979) that the steel should begin strain hardening before the concrete begins to crush, Yakel and Azizinamini analyzed the minimum depth of the neutral axis that was required to develop strain hardening. The study used Equation 2.12 and Equation 2.13 to perform this analysis:

$$D_{\lim} = \frac{\varepsilon_u}{\varepsilon_u + \varepsilon_{sh}} * D_t \qquad \textbf{(Equation 2.12)}$$

$$D^* = \frac{D_{\lim}}{D_p} = 1.4 \qquad \textbf{(Equation 2.13)}$$

Here, ε_u represents the concrete crushing strain, ε_{sh} is the steel hardening strain and D_t is the total depth of the section from the top of the concrete to the bottom of the steel. The ductility parameter for composite beams, D^*, could then be calculated by finding the ratio of the limiting neutral axis depth, D_{lim}, to the actual neutral axis depth at failure, D_p. From the tests conducted, it was shown that a ductility parameter of at least 1.4 was required to provide sufficient ductility to achieve the plastic collapse load. It was also shown that the depth of the neutral axis influenced the behavior of the beam as well. When the neutral axis is above

the compression flange, which is the state most often found in design, the tests found that the current AASHTO specifications are overly conservative.

Because of the unsymmetrical tensile and compressive capacities of wood beams, they can be thought of as composite beams as well. This reinforces the idea that the beam must reach the proportional limit and behave inelastically before the neutral axis will move.

3.0 EXPERIMENT

Deformation testing and analysis were performed on one clear 1”x”1x16” Douglas Fir wood beam, shown in Figure 3.1, one 1”x”1x16” Douglas Fir beam containing a knot at mid-height of the face, shown in Figure 3.2, one 1”x”1x16” Douglas Fir beam containing a knot in compression, shown in Figure 3.3, and one 1”x”1x16” Douglas Fir beam containing a knot in tension, shown in Figure 3.4. The beams were loaded to failure in symmetric four-point bending in order to ensure pure flexure in the mid-section of the beam. The loading setup can be seen in Figure 3.5, and the dimensions of the setup are shown in Figure 3.6.

Figure 3.1: Clear specimen

Figure 3.2: Specimen with a knot at mid-height of the face

Figure 3.3: Specimen with a knot in compression

Figure 3.4: Specimen with a knot in tension

Figure 3.5: Four-Point Loading Set-Up

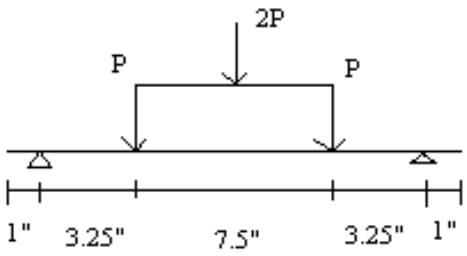

Figure 3.6: Test setup dimensions.

3.1 Specific Methods

Testing was performed using VIC-3D software and Digital Image Correlation equipment. Digital Image Correlation is a non-contact technique used to measure the deformation of an object's surface. Two cameras are angled on the test object and capture a specified number of images every minute depending on the loading rate. The camera setup is shown in Figure 3.7. The VIC-3D software creates a mathematical correlation of the digital images taken during loading. From this correlation, the software can compute surface deformations and strains.

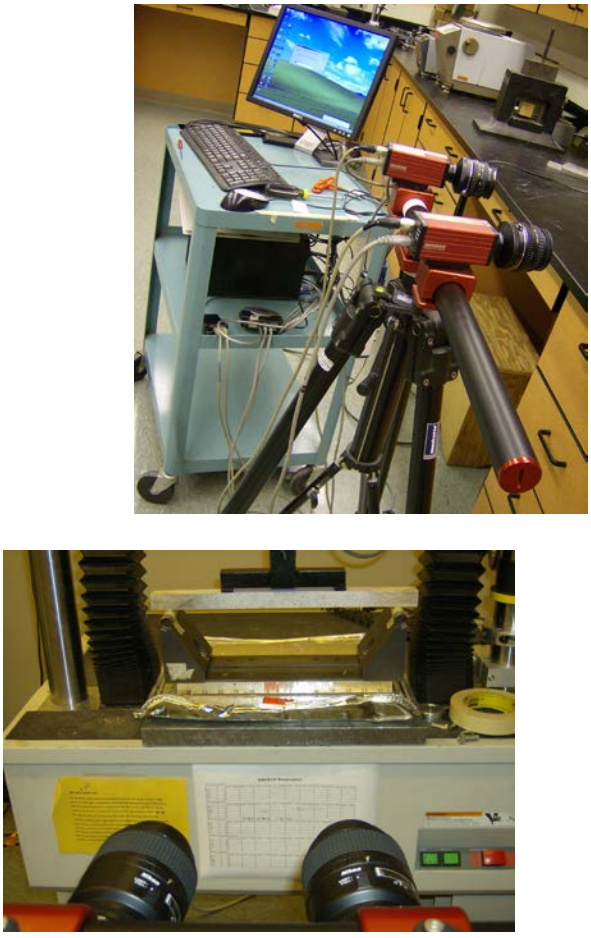

Figure 3.7: DIC Camera Setup

3.1.1 Test Setup

The testing equipment consists of two cameras with high quality lenses. The cameras must be mounted on very stable tripods for measurement accuracy. Additionally, the amount and angle of light on the object must be aligned with the f-stop of the camera to ensure accurate image correlation. The angle between the two cameras should ideally be between 30° and 60°. Much care in test setup is required due to the sensitivity of the cameras and accuracy of

the test. For this experiment, the cameras were set on one side of the tripod and flipped upside down in order to be in line with the test specimen. The front of the camera lens was approximately 16.5 inches away from the beam. It is important to make sure that the camera lenses are clean and free of dust, the cameras are correctly focused on the object and are not moved or touched during testing, the tripods are insensitive to floor vibrations, the lighting is consistent and uniform throughout testing and that the cameras are setup at the correct angle for image collection during testing.

The test object must be sprayed with a random black speckle pattern over a white base, and this is important for accurate results. This speckle pattern is shown in Figure 3.8. It is a trial and error process to determine the type of speckle pattern that will produce good results with the software.

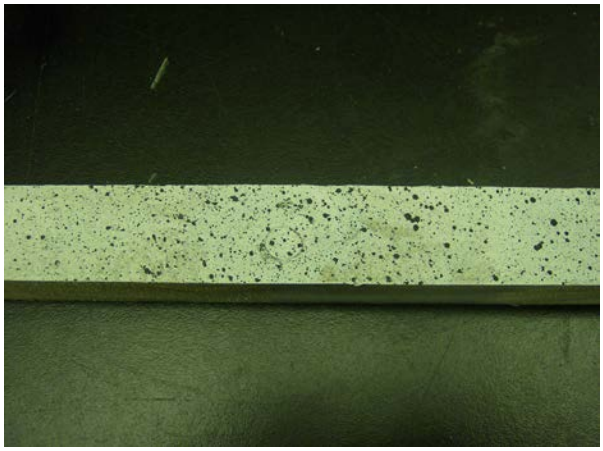

Figure 3.8: Speckle Pattern

After the object surface is sprayed, the cameras can track the pattern during loading. The cameras track this pattern within a specified “Area of Interest”, or AOI. For this experiment, the AOI was defined as a one inch by two inch rectangular area at the center of the beam.

The strains were examined at mid-section of the beam because this is where the greatest stresses are located during bending. The AOI is shown in Figure 3.9.

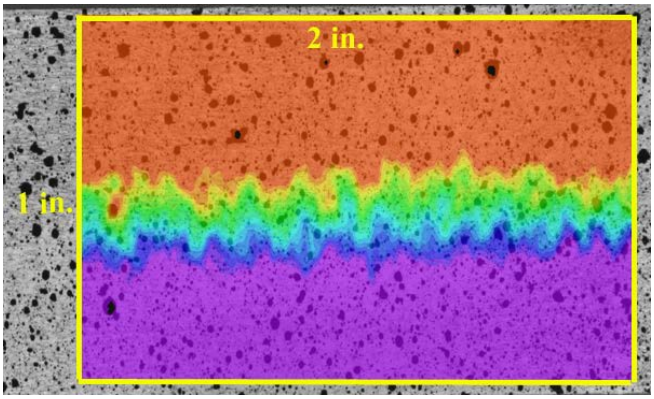

Figure 3.9: Area of Interest, AOI.

Once all test equipment is setup, the VIC-3D software must be setup for testing. This requires a calibration process particular for the test. Images from both cameras are taken of the calibration target at varying orientations. As shown in Figure 3.10, the software needs to recognize three dots on the surface that will be tracked during deformation. The software will display the calibration report which shows the standard deviation for the images acquired and it is important that this deviation is less than 0.1 for precise results. The threshold may need to be adjusted for accurate calibration, or the image may need to be deleted if its error is too large.

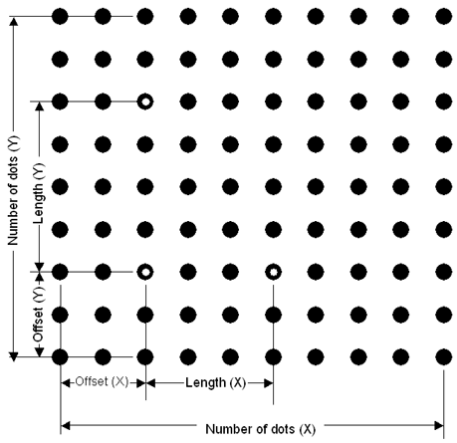

Figure 3.10: Calibration target (VIC-3D Manual)

Once the cameras have successfully been calibrated in the VIC-3D software, the testing can commence. For this test, the beams were loaded at 4mm/min and the images were taken every 2 seconds. Upon failure, the cameras were stopped and the images were retrieved in the VIC-3D software. The image of the object prior to loading, or the reference image, and the images of the specimen under loading, or the deformed images, must be selected. The calibration file can then be imported to the project file. Given that the calibration was successful and the camera setup remains the same for both calibration and testing, the deformed images can be successfully correlated with the calibration images. This means that through the calibration of the cameras, the software can track many locations on the surface of the beam.

3.1.2 Analysis

After the testing has been performed and the deformed images have been correlated through the VIC-3D software, the software can calculate the principal, shear, horizontal and vertical strains from the partial derivatives of the displacement using the LaGrange strain tensor equations (VIC-3D manual). The strain over the area of interest can also be displayed as a

contour plot. Statistics of the accuracy of the reference area can be calculated with VIC-3D as well.

3.2 Expected Results

From the literature review performed for this project and an understanding of the influence of knots, it is evident that the neutral axis in a clear wood beam with plastic behavior will fall below the centroidal axis. How much it will fall in relation to the overall beam depth is still to be analyzed. Additionally, a beam containing knots will affect the movement of the neutral axis depending on their location and size. As explained previously, a knot located at the neutral axis will have very little effect on the strength of the beam. I expect that the neutral axis of a beam with a knot located at the centroid, will behave similarly to that of a clear beam. However, a knot located in the tension zone of the beam will decrease the strength considerably depending on how deep the knot is located. I expect that the neutral axis in a beam with a knot in tension will be significantly higher than that of a clear beam while the neutral axis in a beam with a knot in compression will be significantly lower.

4.0 RESULTS

As shown in Figure 4.2, data from the computer output was checked by plotting the deflection over time for each beam. This plot makes sense because the deflection in the y-direction, V, should be increasing significantly as the load is increase; while the deflections in both the x-direction, U, and the z-direction, W, should not be increasing much since the beam is in bending and the load is only in the y-direction.

The strain in the x-direction corresponding to the deflection at a specific point in time was compared to the theoretical value. The theoretical value was calculated using Equation 4.1, while using Equation 4.2 to calculate the stress, σ, and Equation 4.3 to calculate the modulus of elasticity, E, from the overall beam deflection. The moment, M, was calculated from the load on the beam at the specified point in time, c is the distance from the neutral axis at the mid-section to the extreme compression fiber and the moment of inertia, I, is calculated from the beam geometry. These equations were based on the assumption that the stresses are distributed linearly and symmetrically throughout the cross section. However, this assumption is only valid for wood in the elastic region. Therefore, since each beam reached the proportional limit, and behaved inelastically, this analysis is an estimate and contains some inherent error.

Table 4.1 shows a summary of this data check for the clear beam. The full calculation for the strain check can be found in Appendix A. Naturally, since the beams containing knots are non-homogeneous, the error for these data checks is much larger since the basic assumptions for the use of these equations do not apply to these beams. As stated previously, beams

containing knots only behave elastically initially and exhibit inelastic behavior until failure. Therefore, the elastic assumption of the idealized trapezoidal stress distribution is not valid for beams with knots. Not only this, but since knots decrease the modulus of elasticity of the beam, this would change the theoretical strain value. Because knots in tension affect the modulus of elasticity more so than knots in any other location, the error for the beam with a knot in the tension zone will be greatest.

$$\varepsilon = \frac{\sigma}{E} \qquad \textbf{(Equation 4.1)}$$

$$\sigma = \frac{Mc}{I} \qquad \textbf{(Equation 4.2)}$$

$$E = \left(\frac{Pa}{24\Delta_{mid} I} \right) \left(3L^2 - 4a^2 \right) \qquad \textbf{(Equation 4.3)}$$

Table 4.1: Data check for clear wood beam.

Clear Beam		
ε_{Actual}	$\varepsilon_{Theoretical}$	Percent Error
0.001987	0.0026	30.9

After this data check was done for each beam, data analysis was commenced. Lines to approximate the location of the neutral axis for each of the beams were drawn in order to define the location. Once the neutral axes were drawn, the neutral axis height was calculated as a percentage of the total beam height (one inch). A comparison of the percentage of the height of the neutral axis over the area of interest for each beam is shown in Figure 4.3. Table 4.2 summarizes the location of the neutral axis in each beam. The load versus deflection is plotted in Figure 4.4. Figure 4.5 shows each beam at the same scale in the

elastic state at a total load of approximately 730 N. Figure 4.6 shows the shear strain, e_{xy}, for each beam at failure.

The strain contour plots produced by the VIC-3D software give a clear visual image of where the neutral axis lies in each of the loaded beams. Short movies of the contour plots during loading, Excel output files from VIC-3D, and all tables used for each beam can be found on the CD included with this paper. Specifically, the contour plot of the strain in the x-direction was the focus for this experiment because it displays the strain on the surface of the beam in the horizontal direction. This is important due to the assumption that cross-sections remain plane and normal to the longitudinal axis. Therefore, during deformation, the longitudinal distances between cross-sections either lengthen or shorten except for at the location of the neutral axis. This creates normal strains in the x-direction. In the contour plots, purple represents compression, red is tension, and green is neutral or no strain. The solid green line spanning horizontally through the beam is the neutral axis of the beam. As shown in Figure 4.1, the neutral axis for the different beams varies significantly from each other.

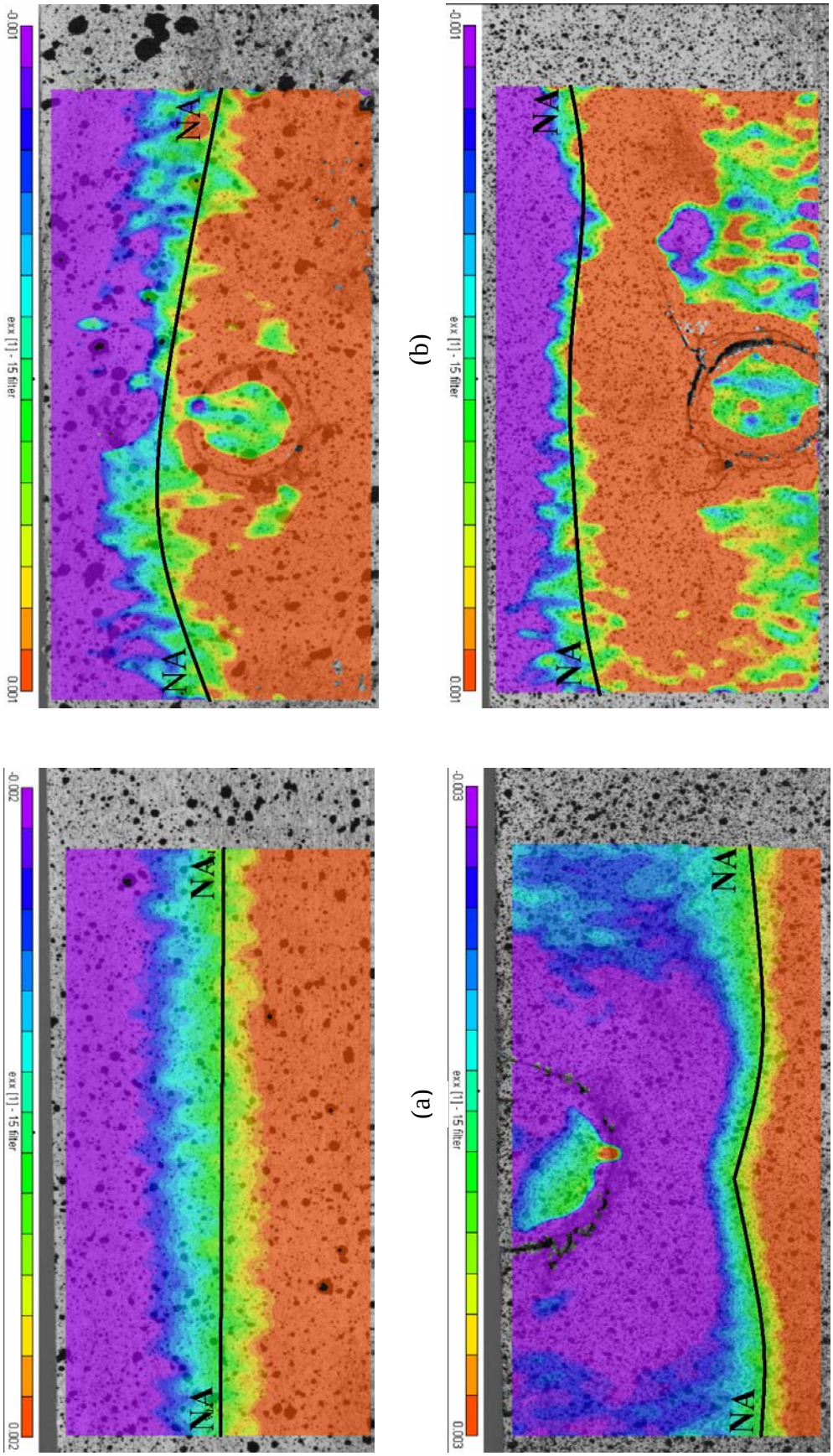

Figure 4.1: Strain (e_{xx}) contour plots just before failure for a (a) Clear beam (b) Knot located at center (c) Knot located in compression zone (d) Knot located in tension zone.

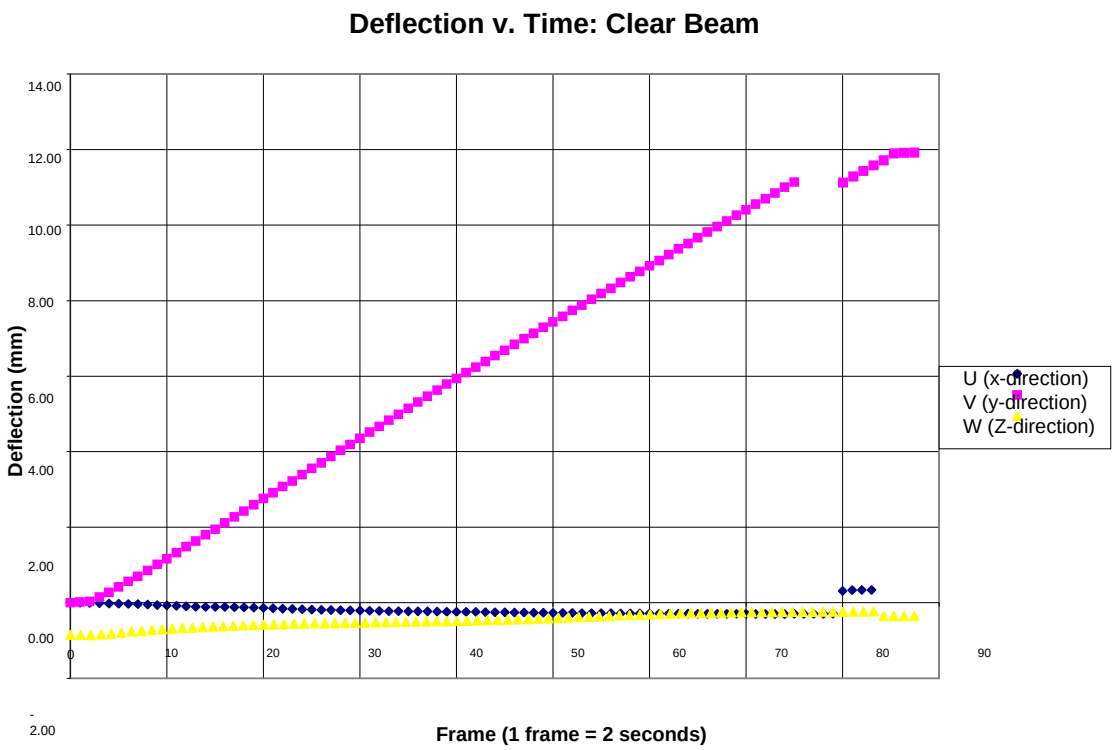

Figure 4.2: Plot of the deflection versus time for the clear beam

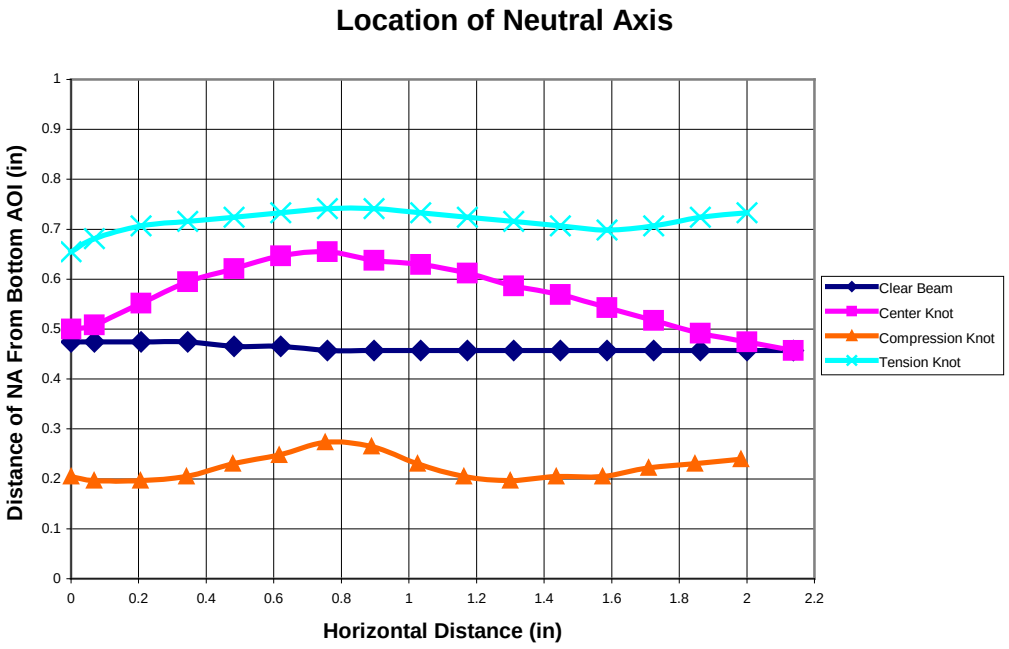

Figure 4.3: Plot of the location of the neutral axis along the area of interest for each beam.

Table 4.2: Location of NA in AOI

	Location of NA From Bottom of AOI (in)*			
Beam	**Left Edge**	**Mid-Section**	**Right Edge**	**Average**
Clear	0.474	0.457	0.457	0.462
Center Knot	0.500	0.612	0.457	0.564
Compression Knot	0.205	0.231	0.239	0.222
Tension Knot	0.655	0.733	0.733	0.715

*AOI = Area of Interest

Load (N)

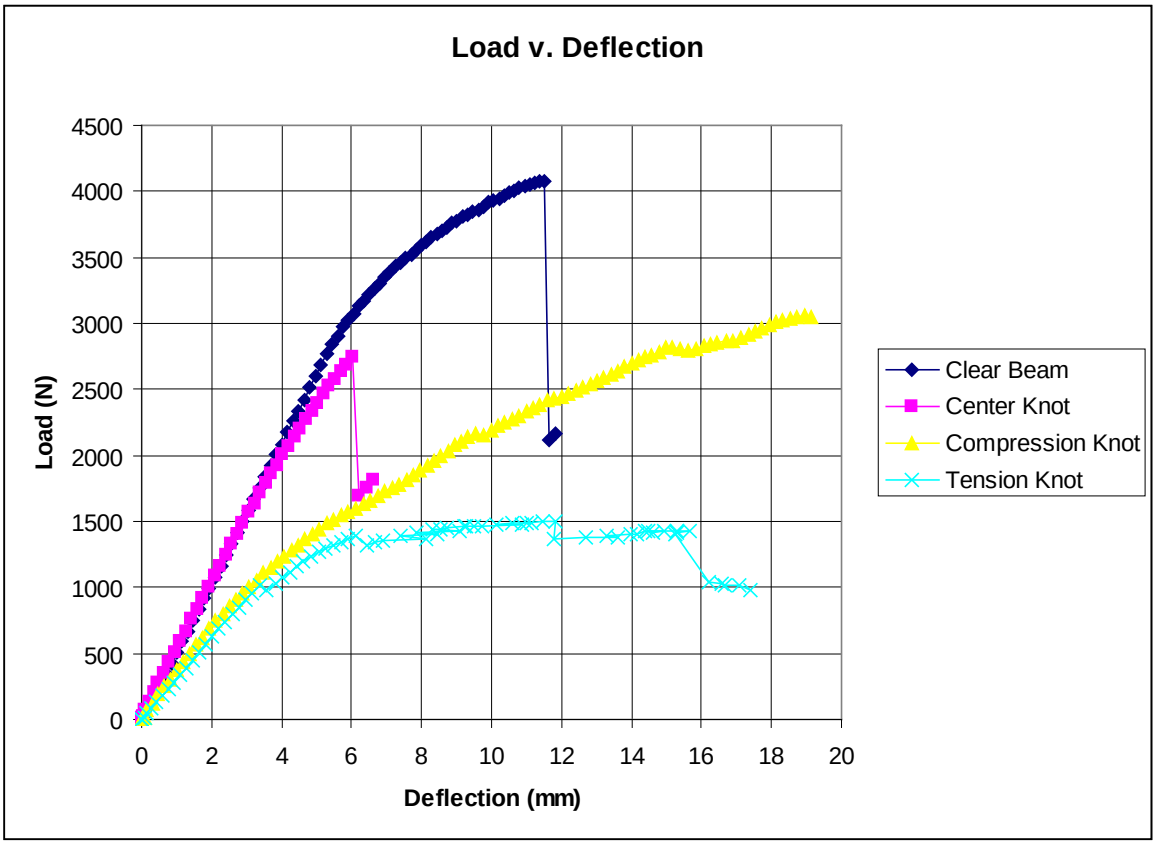

Figure 4.4: Plot of the load versus deflection for each beam

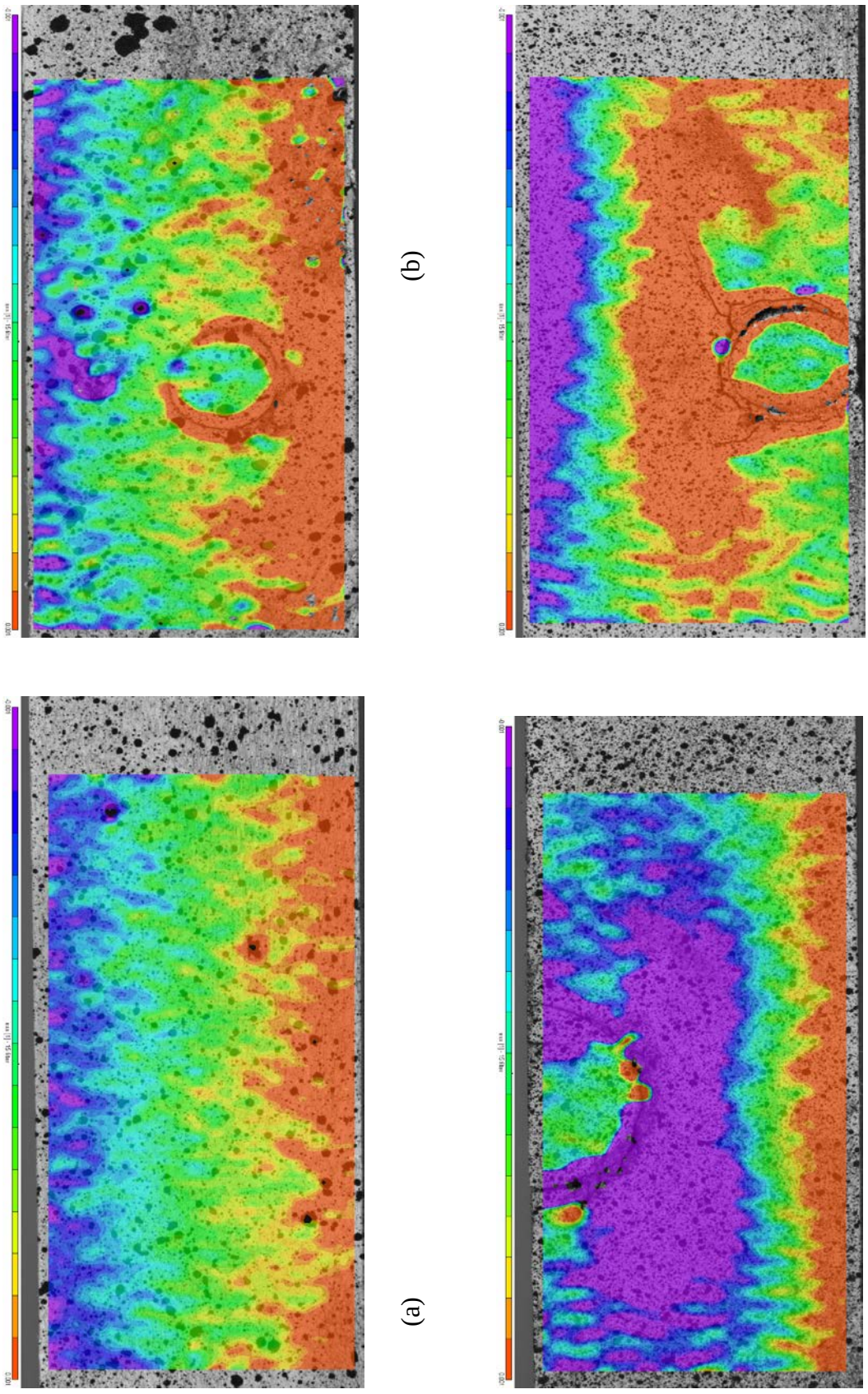

Figure 4.5: Strain (e_{xx}) contour plots at elastic state (total load ≈ 730 N) for a (a) Clear beam (b) Knot located at center (c) Knot located in compression zone (d) Knot located in tension zone

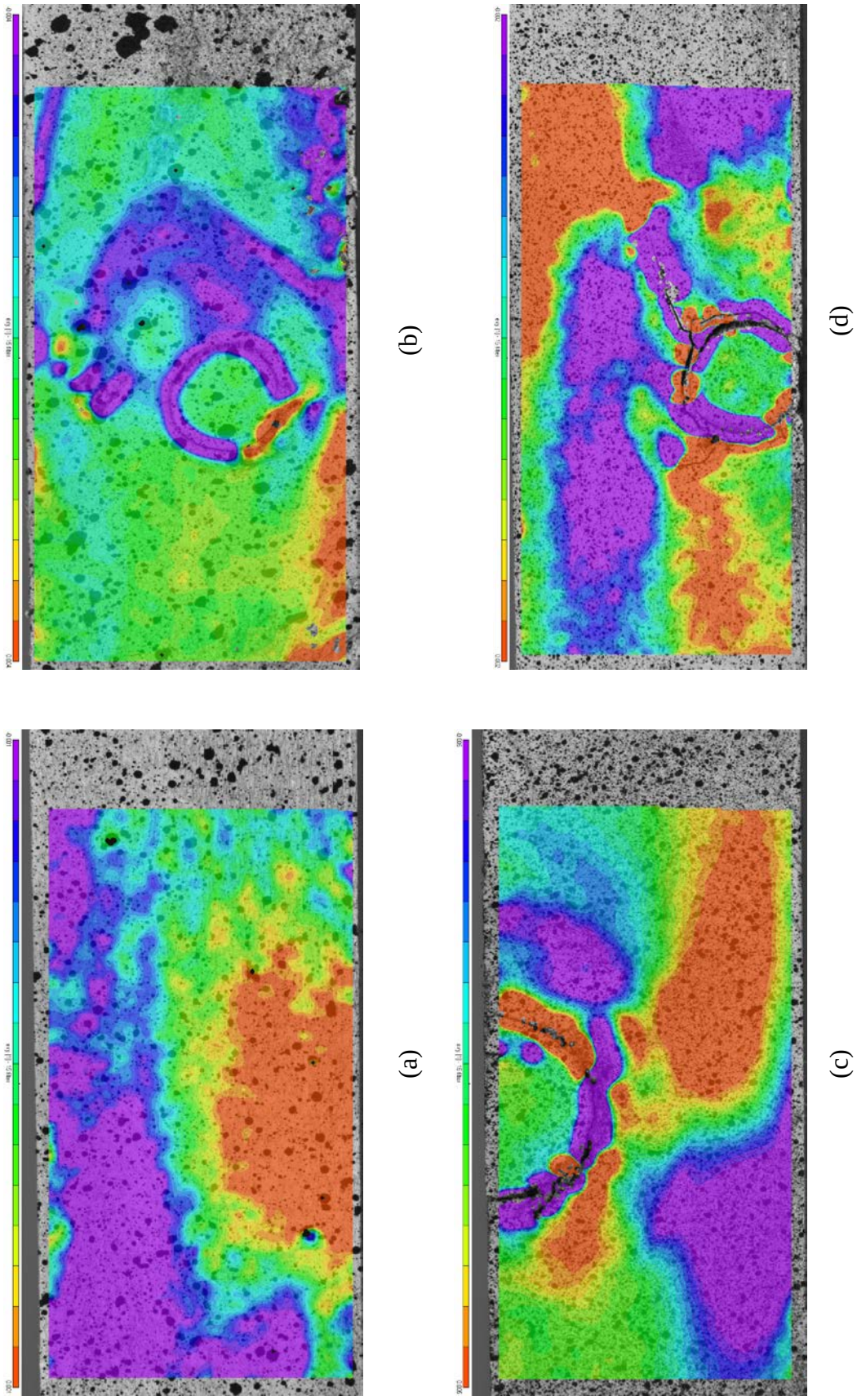

Figure 4.6: Shear strain (e_{xy}) contour plots just before failure for a (a) Clear beam (b) Knot located at center (c) Knot located in compression zone (d) Knot located in tension zone

4.1 Clear Beam

The neutral axis in the clear wood beam performed differently than expected from the literature search. The neutral axis did not seem to move much away from the centroidal axis during loading, although it was expected that the neutral axis would fall below the centroidal axis after reaching the proportional limit. The plot of the location of the neutral axis, shown in Figure 4.3, shows that the neutral axis for the clear beam ranged from 0.457 inches to 0.474 inches from the bottom of the beam just before failure. The beam failed with a tension crack shown in Figure 4.8 at a total load of approximately 4.08 kN. As depicted in Figure 4.7, even up until failure, the neutral axis remained very close to the centroidal axis of the beam. As shown in Figure 4.9, from the strain contour plots, the neutral axis did not seem to move away much from the centroidal axis even after it reached the proportional limit.

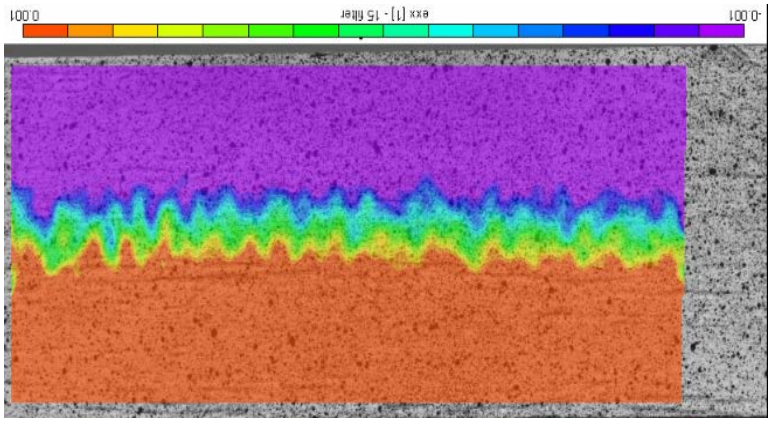

Figure 4.7: Strain (e_{xx}) contour plot for a clear wood beam just before failure at 4.08 kN.

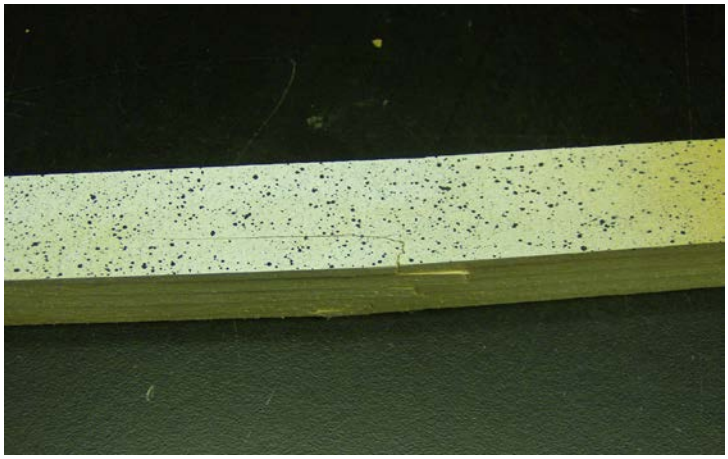

Figure 4.8: Failure crack on tension side for clear beam.

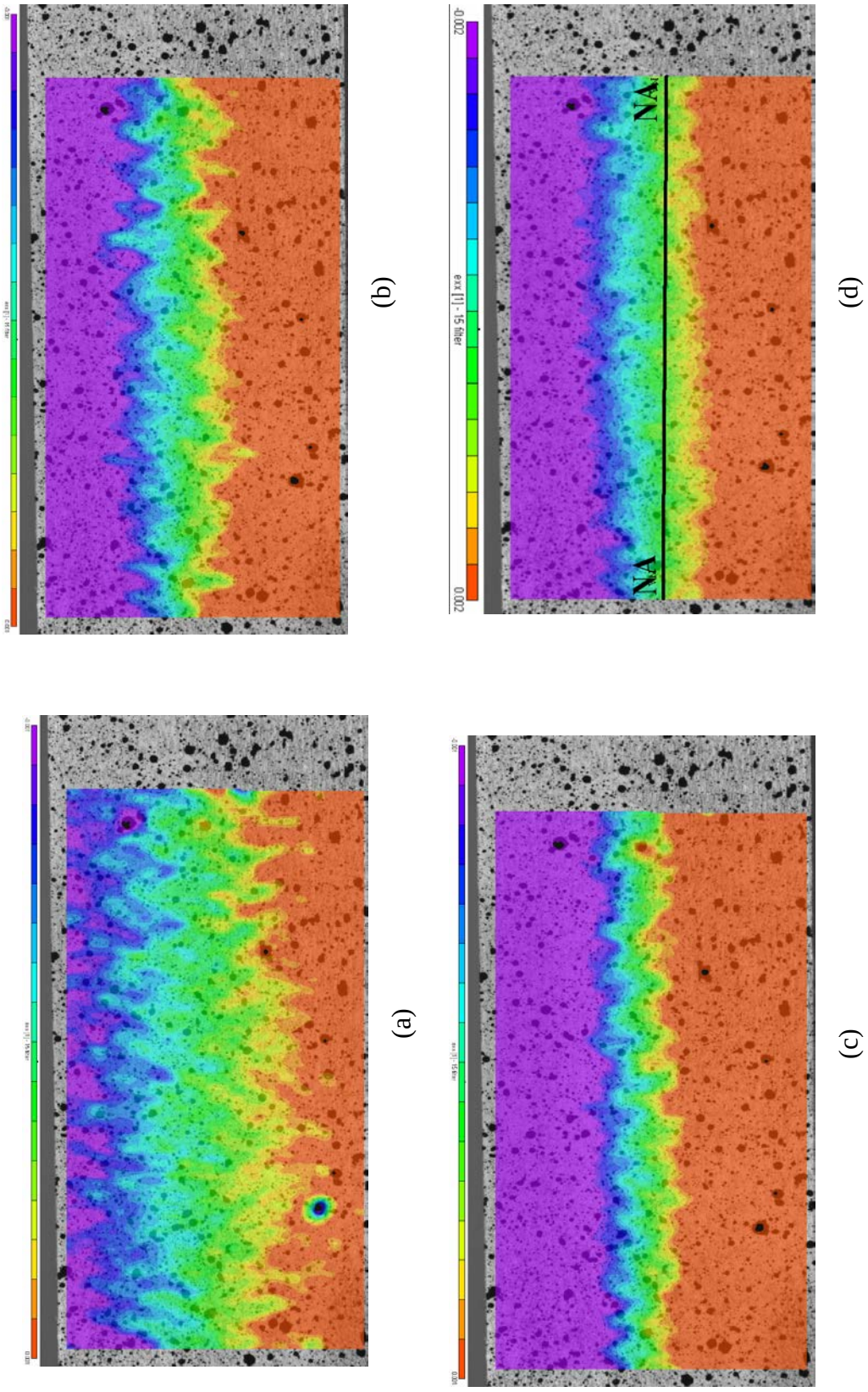

Figure 4.9: Strain (e_{xx}) contour plots for a clear beam under (a) 0.997 kN load (b) 2.01 kN load (c) 3.03 kN load (d) Failure load: 4.08 kN

4.2 Knot at Center

As expected, throughout the loading, the beam with a knot at the center developed a tensile stress concentration around the knot. This is shown in Figure 4.10. In fact, the stress concentrated around the knot first before distributing throughout the beam. This decreased the load capacity, in comparison to the clear beam, by almost 33 percent. The beam failed with a tension crack shown in Figure 4.12 at a total load of approximately 2.74 kN. It is also apparent from the contour plot, shown in Figure 4.11, that there is little to no stress in the middle of the knot. This is because the knot is an encased knot and is therefore slightly detached from the rest of the beam.

The average location of the neutral axis is approximately 0.10 inches above the neutral axis for the clear beam. However, the variation of the neutral axis along the length of the beam is very different. As can be seen in Figure 4.3 and described in Table 4.2, the neutral axis begins on the left side of the area of interest at approximately the same location as in the clear beam. However, as the neutral axis moves toward the knot at the center of the area, it rises above the knot to about 0.61 inches from the bottom of the beam. Finally, towards the right side of the area, the neutral axis moves back toward the centroidal axis and ends up at the same height as that of the clear beam at that location. This shows that the neutral axis in the beam with a knot located at the centroid behaves like a clear beam away from the knot, but will move around the knot at the mid-section. In this test, the neutral axis moved toward the compression zone of the beam, however, the knot is slightly lower than the centroid on the beam. It would be interesting to look at a beam with the knot either at the exact location of the centroid, or slightly above the centroid, to see if the neutral axis moves toward the

compression zone again. The strain contour plots at different loads for the beam with the knot located at the center can be found in Appendix B.

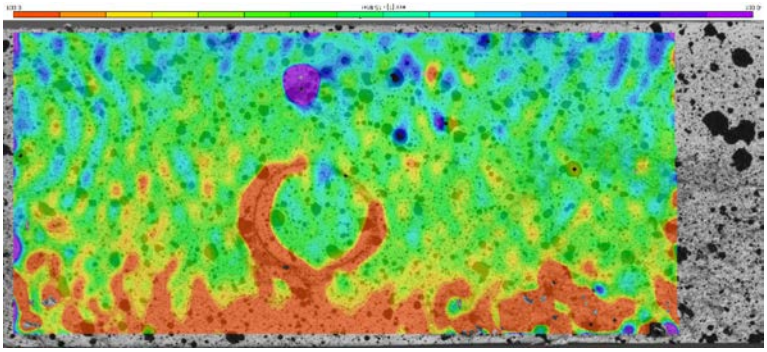

Figure 4.10: Stress concentration at knot in elastic region.

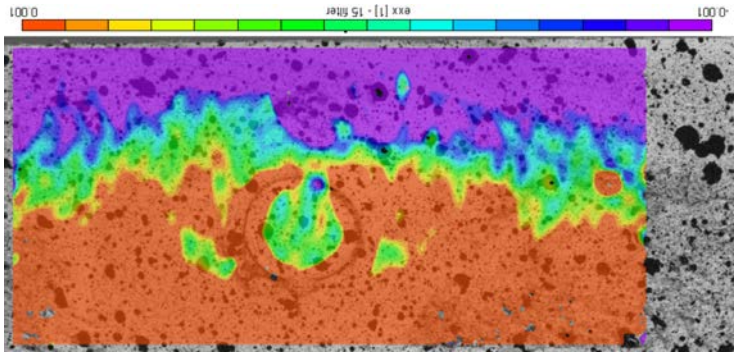

Figure 4.11: Strain (e_{xx}) contour plot for a wood beam with a knot at the center just before failure at 2.74 kN.

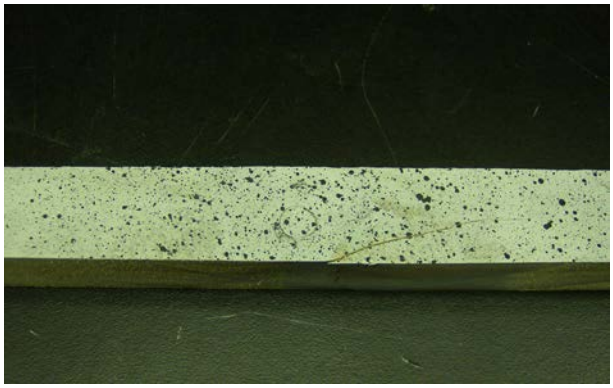

Figure 4.12: Failure crack on tension side for beam with a knot at the center.

4.3 Knot in Compression Zone

Again, the beam developed a stress concentration around the knot throughout loading; however, this knot seemed to be more connected to the beam because the stress distributed more evenly through the knot, as shown in Figure 4.13. There is only a small section in the center of the knot that has almost no stress. Again the load capacity was significantly reduced. The beam with the knot in compression failed at a load of approximately 3.06 kN. This is a 25 percent reduction in strength as compared to the clear beam. As shown in Figure 4.14, the beam actually failed at the location of the knot. A crack developed through the knot and progressed through the cross section of the beam in the compression zone.

As summarized in Table 4.2 and plotted in Figure 4.3, the neutral axis shifted significantly away from the centroidal axis. The average location of the neutral axis was only 0.22 inches from the bottom of the beam. The neutral axis started at approximately 0.21 inches from the

bottom at the left edge of the area of interest and it remained relatively straight along the distance of the beam. However, at the location of the knot, the neutral axis actually moved up toward the knot, and was at 0.23 inches from the bottom. This is different from the neutral axis for the beam with the knot at the center where the neutral axis moved away from the knot at the mid-section. The strain contour plots at different loads for the beam with the knot located in the compression zone can be found in Appendix B.

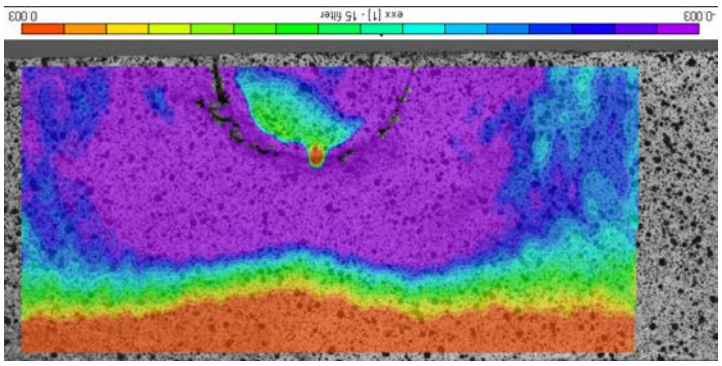

Figure 4.13: Strain (e_{xx}) contour plot for a wood beam with a knot in compression just before failure at 3.06 kN.

Figure 4.14: Failure crack on compression side for beam with a knot in the compression side.

4.4 Knot in Tension Zone

This beam behaved nearly opposite to the beam with the knot in the compression zone. While the knot in the compression zone caused the neutral axis to move about 0.28 inches below the centroidal axis, the knot in the tension zone caused the neutral axis to move about 0.22 inches above the centroidal axis. As shown in Figure 4.16, it also developed a stress concentration around the knot and the majority of the center of the knot had little to no stress. The beam's strength was the most significantly reduced, failing at a load of only 1.40 kN. This is nearly a 66 percent reduction in strength compared to the clear beam. Again, the beam failed at the location of the knot as shown in Figure 4.15. The knot nearly cracked out of the beam during failure.

The neutral axis behaved very similarly to that of the compression beam. It moved considerably away from the knot as well. As depicted in Figure 4.3 and summarized in Table 4.2, the average location of the neutral axis was at about 0.72 inches above the bottom of the beam. It remained relatively straight, starting at 0.66 inches at the left side of the area of interest and ending at 0.73 inches at the right side. The main difference was that at the location of the knot, the neutral axis did not seem to move away or toward the knot. It did, however, drop toward the tension zone slightly after the mid-section. The strain contour plots at different loads for the beam with the knot located in the tension zone can be found in Appendix B.

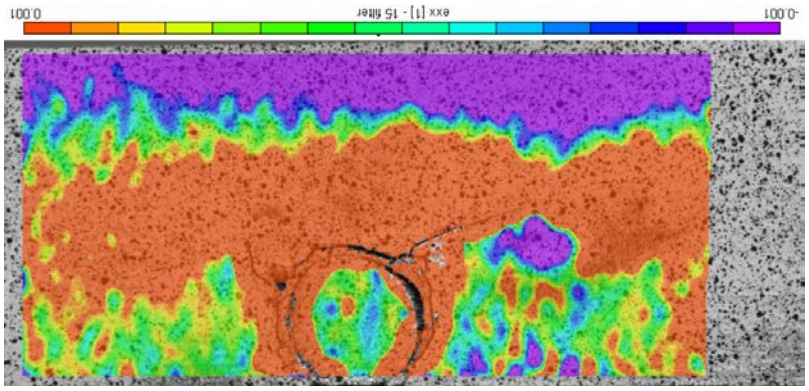

Figure 4.15: Strain (e_{xx}) contour plot for a wood beam with a knot in tension just before failure at 1.40 kN.

Figure 4.16: Failure crack on tension side for beam with a knot at the tension side.

5.0 DISCUSSION AND CONCLUSIONS

The output from the VIC-3D digital imaging correlation software provided a clear image of the location of the neutral axis. The neutral axis in the clear beam remained close to the centroidal axis throughout loading. Even after reaching the proportional limit, the average location of the neutral axis remained at about 0.46 inches from the bottom of the beam. That's only 0.04 inches lower than the centroidal axis. The clear beam followed the idealized stress distribution defined by Kollmann and Cote (1968) shown in Figure 5.1. As stated previously, from the idealized trapezoidal stress distribution, the expected location of the neutral axis was 0.44 inches from the bottom of the beam. The actual location of the neutral axis was approximately 0.46 inches from the bottom of the beam. Again, since this idealized distribution assumes elastic behavior, there is a slight amount of error due to the inelastic behavior of the clear beam just before failure.

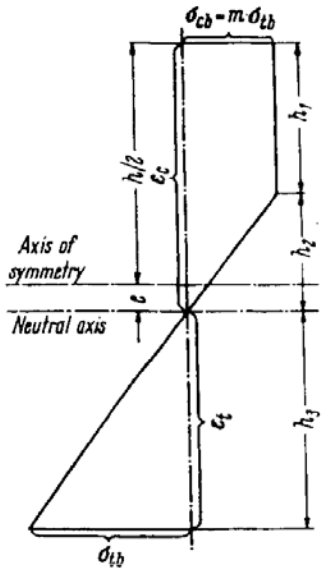

Figure 5.1: Stress Diagram for Trapezoid-like Distribution of the Stresses Over the Cross-Section of a Wood Beam (Kollmann and Cote 1968)

From the literature search, it was expected that the neutral axis would move away from the centroidal line after the proportional limit was reached. The small difference between the expected location of the neutral axis, determined from the idealized stress distribution, and the actual location of the neutral axis just before failure may account for the movement of the neutral axis after the proportional limit has been reached. However, from the strain contour plots, it is difficult to determine whether the neutral axis moved much during loading.

Unfortunately, there is no idealized stress distribution that can be used for beams containing knots because the stresses around the knots are very complex and not well understood. From testing it is apparent that the location of the knot within the beam determines the size of the compression and tension zones as well as the location of the neutral axis. Beams with knots at the center will usually have a neutral axis near the centroidal axis, as in the clear beam, except at the location of the knot. At this location, the neutral axis moves away from the centroidal axis and moves around the knot. This may be due to the fact that the knot in this beam is actually located slightly lower than the centroidal axis as shown in Figure 5.2. Therefore, because the knot reduces the modulus of elasticity, this causes the tensile strain to increase, pushing the neutral axis above the centroidal axis.

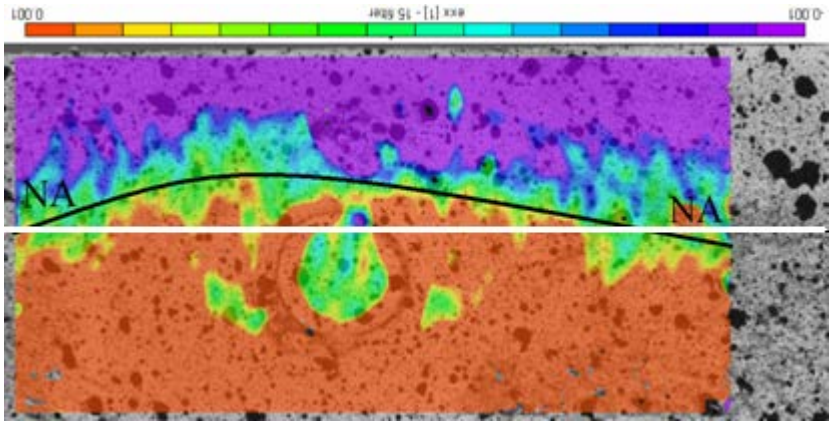

Figure 5.2: Location of Center Knot Below the Centroidal Axis (White Line)

For a beam with a knot in tension, the neutral axis moved approximately 0.22 inches away from the centroidal axis toward the compression zone. For a beam with a knot in compression, the neutral axis moved approximately 0.28 inches away from the centroidal axis toward the tension zone. The cause of this may be because, again, the knot lowers the effective modulus of elasticity at the location of the knot. For the beam with the knot in compression, the knot reduced the modulus of elasticity causing the compressive strain to increase. This causes the neutral axis to shift much lower than the centroidal axis closer to the tensile zone. The reverse is true for the beam with the knot located in the tension zone. Additionally, as explained previously, the location of the knot also affects the strength of the beam. Knots located in the tension zone will cause a greater strength reduction than those located in the compression zone.

6.0 FUTURE WORK

As this project progressed, it was apparent that there were many things not covered within its scope that needed to be examined in more depth. The beams that were examined in this paper were only four of ten that were tested. The other beams that were tested were another clear Douglas Fir beam, one clear Oak beam, one beam with a hole drilled through the center, one beam with a hole drilled in the compression zone, one beam with a hole drilled in the tension zone, and one beam with a hole drilled through the center of the face perpendicular to loading. Because these beams were tested and the data has been collected, it would be important for further analysis to be done on these beams for comparison with the beams discussed in this paper. For example, it would be interesting to see how the beam with a hole drilled through the center of the face would compare to the beam with the knot in the center. Because the knot was encased, or somewhat disconnected to the surrounding wood fibers, I would expect the results to be similar.

As discussed previously, all the knots in this project were encased knots. Encased knots are somewhat disconnected from the surrounding wood fibers of the beam, while intergrown knots are completely connected to the beam but create more cross-grain in the beam. Because of this, there were stress concentrations around the knot, but nearly no stress in the middle of the knot. Encased knots generally resist little to no stress. The neutral axis always moved around the knot, never through the knot. This is especially significant for knots at the center of the beam since the neutral axis moves from the centroidal axis to go around the knot at the center. Intergrown knots tend to affect mechanical properties of wood more than encased knots, although both types of knots reduce the strength of the wood similarly. It

would be important to look at intergrown knots to see if the stress distributes more evenly through the knot and how this would affect the location of the knot.

Finally, a more complex analysis of the data would be appropriate in order to develop empirical equations to determine the neutral axis of the beams containing knots. These equations would obviously be dependent on the location of the knot and would lead to a much better prediction of the behavior of such beams during loading.

BIBLIOGRAPHY

Bažant, Z. and Jirásek, M. (2002). *Inelastic Analysis of Structures.* John Wiley & Sons, Ltd. West Sussex, England. pp. 351-353.

Boresi, A., Schmitdt, R., and Sidebottom, O. (1993). *Advanced Mechanics of Materials* (5th Edition). John Wiley & Sons, Inc. New York, NY. pp.90-93.

Correlated Solutions. (2005). *Vid-3D User Manual.* Correlated Solutions, Inc. Columbia, SC.

Craig, R. (1996) *Mechanics of Materials.* John Wiley & Sons, Ltd West Sussex, England. pp. 296-297

Forest Products Laboratory (1992). *Wood as A Structural Material.* The Pennsylvania State University, University Park, Pa, 94 pages.

Forest Products Laboratory (1999). *Wood Handbook: Wood as an Engineering Material. General Technical Report 113.* U.S. Department of Agriculture, Forest Service, Forest Products Laboratory, Madison, WI. 463 pages.

Gere, J. and Timoshenko, S. (1997). *Mechanics of Materials* (4th Edition). PWS Pub. Co., 912 pages.

Kollmann F. and Cote, W. (1968). *Principles of Wood Science and Technology I: Solid Wood.* Springerverlag, New York. 419 pages.

Lopes, S. and Bernardo, L. (2004). "Neutral Axis Depth Versus Flexural Ductility in High-Strength Concrete Beams." *Journal of Structural Engineering,* ASCE 130(3), 452-459.

Redler, H. "Movement of Neutral Axis in Beams Subjected to Pure Bending." Submitted for a Reading and Conference class to Dr. Rakesh Gupta at Oregon State University. Corvallis, OR.

Rotter, J. M., and Ansourian, P. (1979). "Cross-Section Behavior and Ductility in Composite Beams." *Proc., Inst. Of Civil Engineers, Part 2* Vol., 67, 453-474.

Somayaji, S. (2001). *Civil Engineering Materials* (2nd Edition). Prentice Hall. 468 pages.

Yakel, A. and Azizinamini, A. (2005). "Improved Moment Strength Prediction of Composite Steel Plate Girders in Positive Bending." *Journal of Bridge Engineering,* ASCE 10(1), 28-38.

APPENDICES

Appendix A: Strain Data Check

Appendix B: Strain Plots at Different Loading

Appendix A:

Strain Data Check

Strain Check: Clear Beam

- From VIC-3D software:

Strain in elastic behavior at mid-span and extreme compression fiber: $\mathbf{e_{xx} = 0.0019781}$

- For four-point bending:

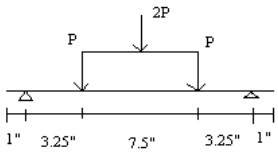

$$\Delta_{mid} = \left(\frac{Pa}{24EI}\right)\left(3L^2 - 4a^2\right)$$

Where: a = 3.25 in.
P = 709.8 N
Δ_{mid} = 0.00276 mm (from VIC 3-D)
L = 14 in.
I = 0.0833 in^4

- Therefore,

$$E = \left(\frac{Pa}{24\Delta_{mid} I}\right)\left(3L^2 - 4a^2\right)$$

E = 8.97 GPa

- Bending stress:

$$\sigma = \frac{Mc}{I}$$

- From statics, moment(in N-m) at mid-span:

$$M = .08255P$$

M = 58.6 N-m

- c = distance from neutral axis to extreme compression fiber

c = 0.543 in

- Therefore,

σ = 23.3 MPa

- Strain:

$$\varepsilon = \frac{\sigma}{E} = \frac{0.0196}{8.97} = 0.0022$$

Clear Beam		
ε_{Actual}	$\varepsilon_{Theoretical}$	Percent Error
0.001987	0.0026	30.9

Strain Check: Center Knot Beam

- From VIC-3D software:

Strain in elastic behavior at mid-span and extreme compression fiber: **e_{xx} = 0.0042608**

- For four-point bending:

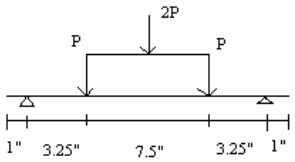

$$\Delta_{mid} = \left(\frac{Pa}{24EI}\right)\left(3L^2 - 4a^2\right)$$

Where: a = 3.25 in.
P = 664.4 N
Δ_{mid} = 0.00257 mm (from VIC 3-D)
L = 14 in.
I = 0.0833 in^4

- Therefore,

$$E = \left(\frac{Pa}{24\Delta_{mid} I}\right)\left(3L^2 - 4a^2\right)$$

E = 9.02 GPa

- Bending stress:

$$\sigma = \frac{Mc}{I}$$

- From statics, moment(in N-m) at mid-span:

$$M = .08255P$$

M = 54.8 N-m

- c = distance from neutral axis to extreme compression fiber

c = 0.388 in

- Therefore,

σ = 15.6 MPa

- Strain:

$$\varepsilon = \frac{\sigma}{E} = \frac{0.0156}{9.02} = 0.001728$$

Center Knot Beam		
ε_{Actual}	$\varepsilon_{Theoretical}$	Percent Error
0.004261	0.0017277	59.5

Strain Check: Compression Knot Beam

- From VIC-3D software:

Strain in elastic behavior at mid-span and extreme compression fiber: $\mathbf{e_{xx} = 0.002546}$

- For four-point bending:

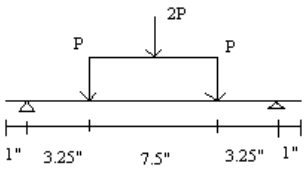

$$\Delta_{mid} = \left(\frac{Pa}{24EI}\right)\left(3L^2 - 4a^2\right)$$

Where: a = 3.25 in.
P = 504.3 N
Δ_{mid} = 0.00308 mm (from VIC 3-D)
L = 14 in.
I = 0.0833 in^4

- Therefore,

$$E = \left(\frac{Pa}{24\Delta_{mid} I}\right)\left(3L^2 - 4a^2\right)$$

E = 5.72 GPa

- Bending stress:

$$\sigma = \frac{Mc}{I}$$

- From statics, moment(in N-m) at mid-span:

$$M = .08255P$$

M = 41.6 N-m

- c = distance from neutral axis to extreme compression fiber

c = 0.769 in

- Therefore,

σ = 23.4 MPa

- Strain:

$$\varepsilon = \frac{\sigma}{E} = \frac{0.0234}{5.72} = 0.0040971$$

Compression Knot Beam		
ε_{Actual}	$\varepsilon_{Theoretical}$	Percent Error
0.002546	0.0040971	60.9

Strain Check: Tension Knot Beam

- From VIC-3D software:

Strain in elastic behavior at mid-span and extreme compression fiber: $\mathbf{e_{xx} = -0.00053}$

- For four-point bending:

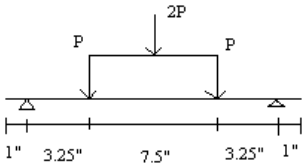

$$\Delta_{mid} = \left(\frac{Pa}{24EI}\right)\left(3L^2 - 4a^2\right)$$

Where: a = 3.25 in.
P = 354.9 N
Δ_{mid} = 0.00317 mm (from VIC 3-D)
L = 14 in.
I = 0.0833 in^4

- Therefore,

$$E = \left(\frac{Pa}{24\Delta_{mid} I}\right)\left(3L^2 - 4a^2\right)$$

E = 3.91 GPa

- Bending stress:

$$\sigma = \frac{Mc}{I}$$

- From statics, moment(in N-m) at mid-span:

$$M = .08255P$$

M = 29.3 N-m

- c = distance from neutral axis to extreme compression fiber

c = 0.267 in

- Therefore,

σ = 5.73 MPa

- Strain:

$$\varepsilon = \frac{\sigma}{E} = \frac{0.0573}{3{,}91} = 0.001463$$

Tension Knot Beam		
ε_{Actual}	$\varepsilon_{Theoretical}$	Percent Error
-0.00053	0.0014633	-376.1

Appendix B:
Strain Contour Plots During Loading

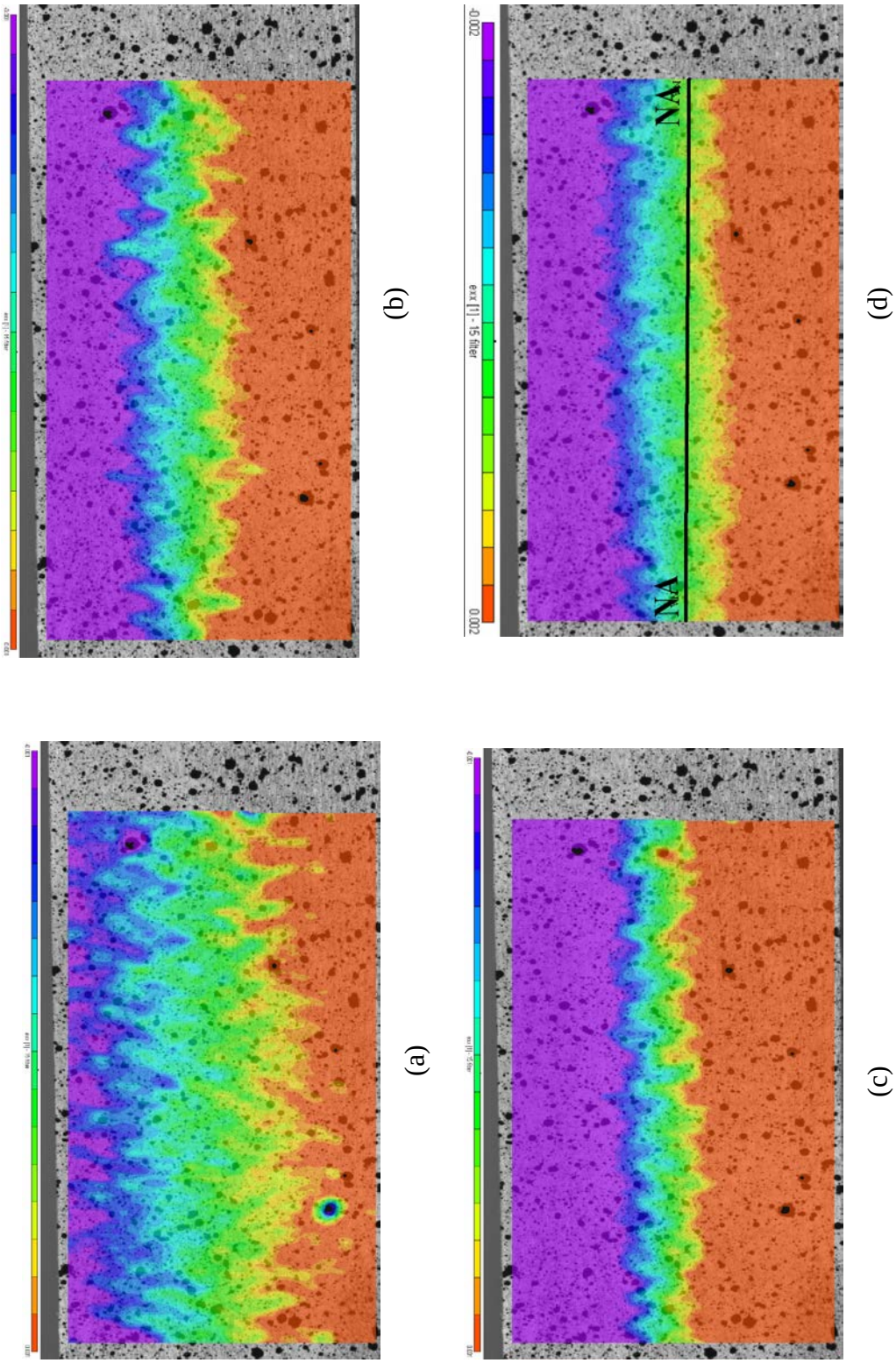

Figure B.1: Strain (e_{xx}) contour plots for a clear beam under (a) 0.997 kN load (b) 2.01 kN load (c) 3.03 kN load (d) Failure load: 4.08 kN

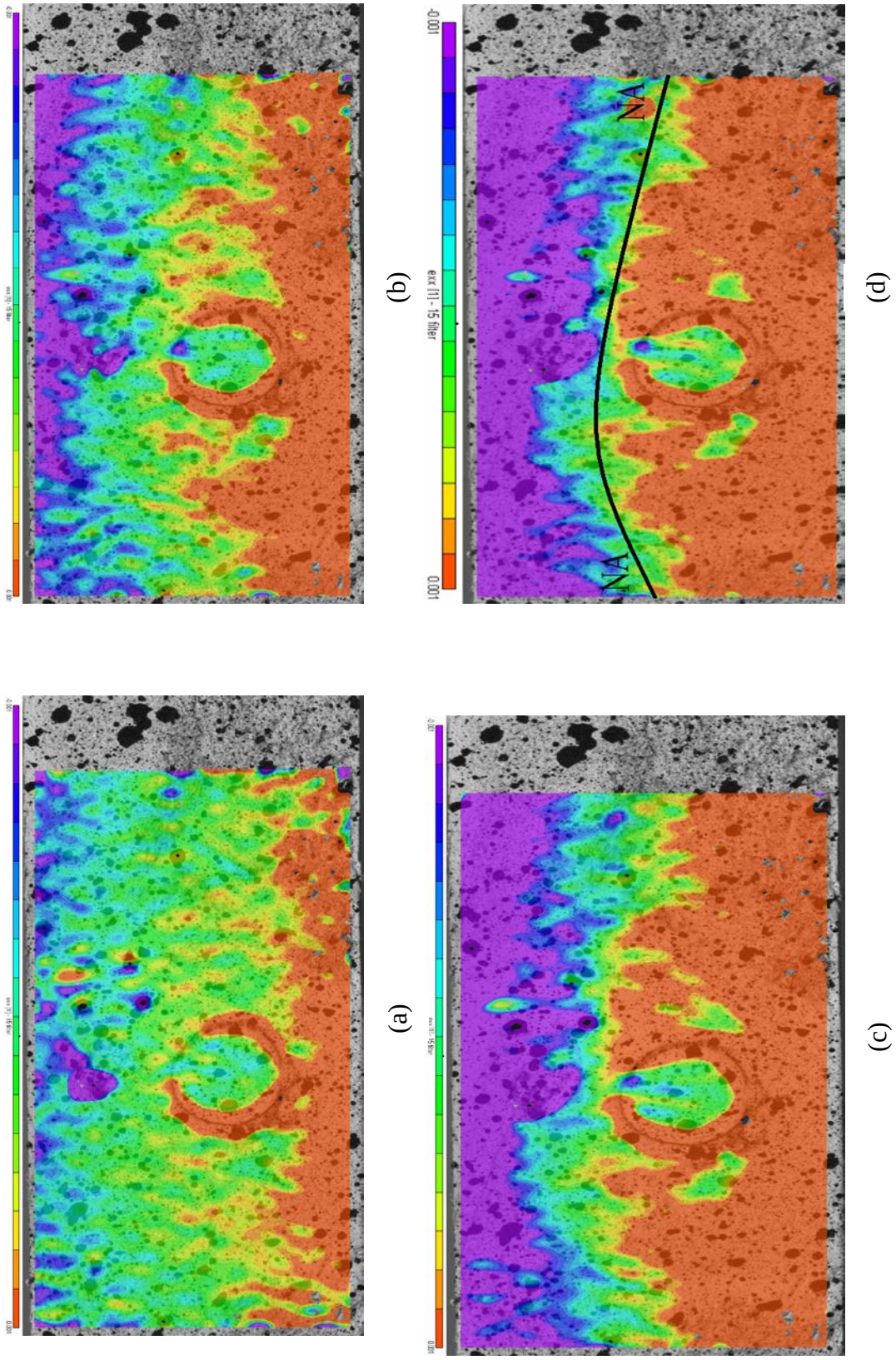

Figure B.2: Strain (e_{xx}) contour plots for a beam with a knot at center under (a) 0.514 kN load (b) 1.00 kN load (c) 2.00 kN load (d) Failure load: 2.74 kN

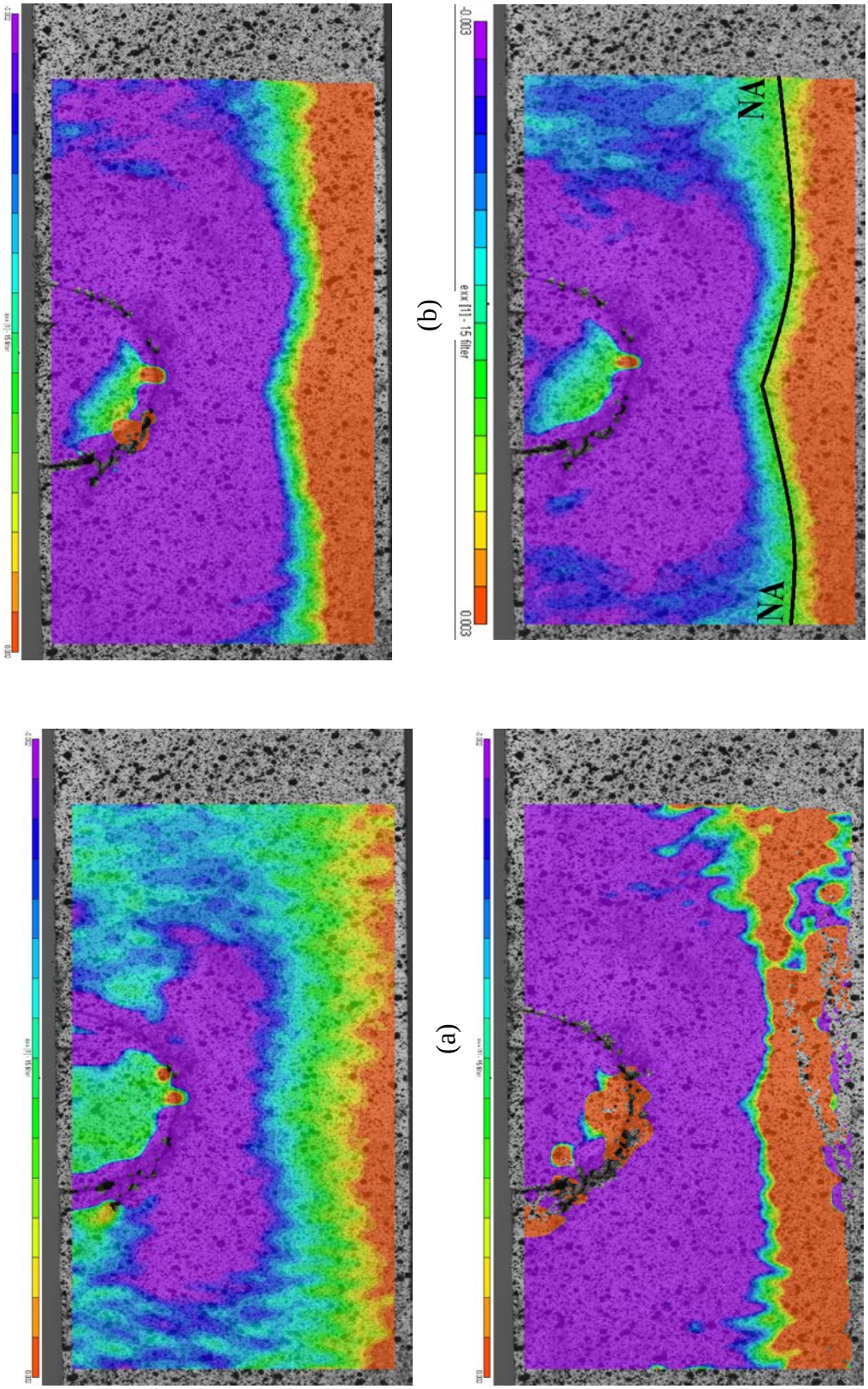

Figure B.3: Strain (e_{xx}) contour plots for a beam with a knot in compression under (a) 1.01 kN load (b) 2.00 kN load (c) 3.00 kN load (d) Failure load: 3.06 kN

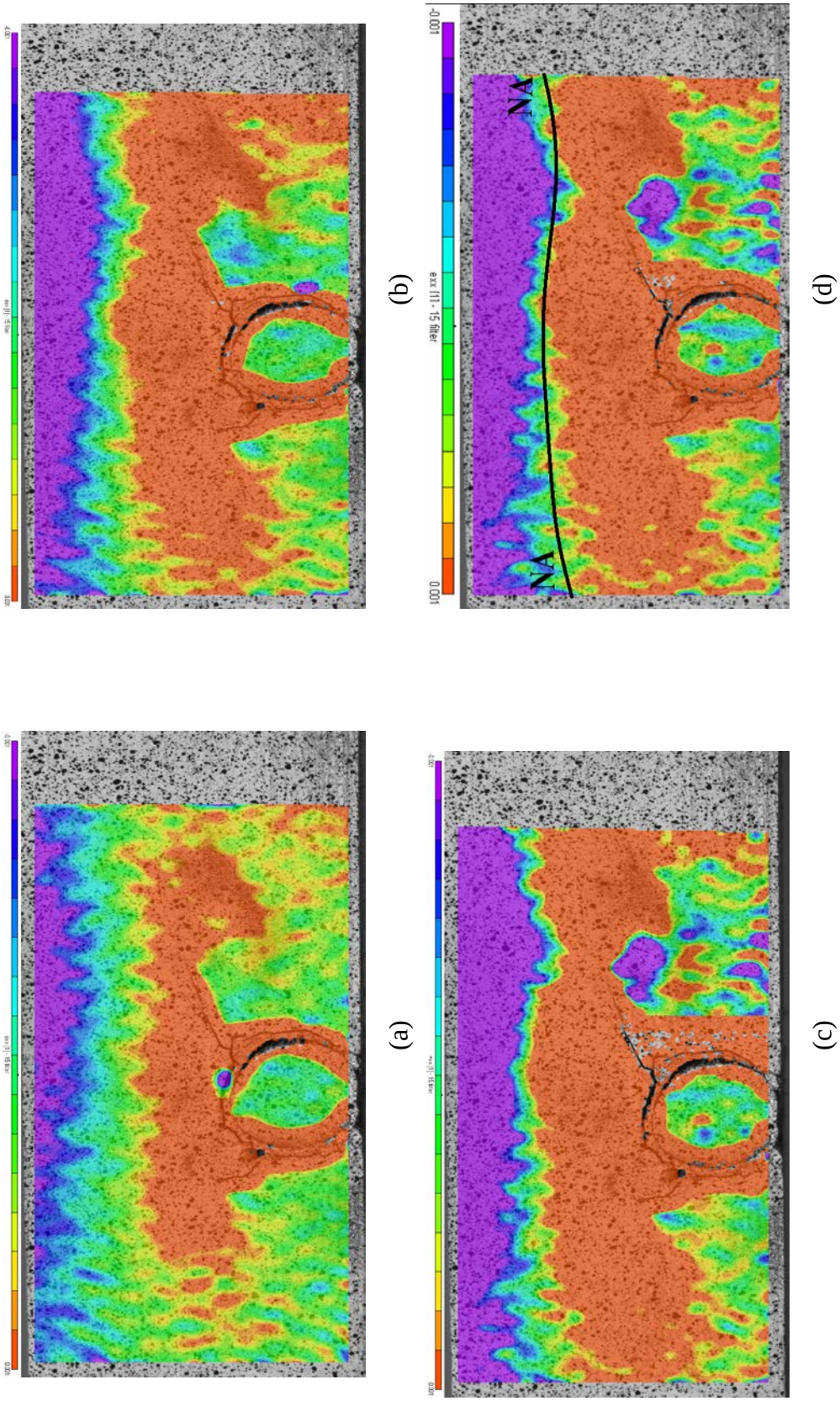

Figure B.4: Strain (e_{xx}) contour plots for a beam with a tension knot under (a) 0.506 kN load (b) 1.01 kN load (c) 1.29 kN load (d) Failure load: 1.40